

EVALUATION OF CONCRETE CONTAINING
PHOTOCATALYTIC TITANIUM DIOXIDE

by

Shannon Hanson

A dissertation submitted to the faculty of
The University of Utah
in partial fulfillment of the requirements for the degree of

Doctor of Philosophy

Department of Civil and Environmental Engineering

The University of Utah

May 2014

Copyright © Shannon Hanson 2014

All Rights Reserved

The University of Utah Graduate School

STATEMENT OF DISSERTATION APPROVAL

The dissertation of Shannon Hanson
has been approved by the following supervisory committee members:

<u>Chris Pantelides</u>	, Chair	<u>12/2/2013</u> Date Approved
-------------------------	---------	-----------------------------------

<u>Larry Reaveley</u>	, Member	<u>12/2/2013</u> Date Approved
-----------------------	----------	-----------------------------------

<u>Paul Tikalsky</u>	, Member	<u>12/2/2013</u> Date Approved
----------------------	----------	-----------------------------------

<u>Amanda Bordelon</u>	, Member	<u>12/2/2013</u> Date Approved
------------------------	----------	-----------------------------------

<u>JoAnn Lighty</u>	, Member	<u>12/2/2013</u> Date Approved
---------------------	----------	-----------------------------------

<u>Tyson Rupnow</u>	, Member	<u>12/2/2013</u> Date Approved
---------------------	----------	-----------------------------------

and by Michael Barber, Chair of
the Department of Civil and Environmental Engineering

and by David B. Kieda, Dean of The Graduate School.

ABSTRACT

The air pollution inversions in the mountain west are a societal problem that require a large-scale solution. With the more stringent Environmental Protection Agency (EPA) regulations established in 2010, and the recent discovery of the photocatalytic pollution reduction capabilities of titanium dioxide (TiO_2), interest has developed to create pollution-reducing construction materials. Over the last decade, a number of laboratory studies have been performed and a few field studies have occurred around the world. There are commercially available photocatalytic materials that can be used in concrete construction; however, the materials are often cost prohibitive. This study investigated both practical application techniques and the effects of the climatic environment around the specimens.

When concrete specimens were exposed to the weather for 120-days, the specimen's photocatalytic efficiency decreased significantly. Rejuvenation methods were investigated; however, no methods tested were able to increase the photocatalytic efficiency of the specimens to preweathered condition.

The final element of this study focused on identifying practical and cost-effective methods of adding TiO_2 to current production methods by working with a local precast manufacturer.

This research is a stepping stone to develop methodologies to minimize the decline of photocatalytic efficiency due to the exposure to the environment. This element is critical in understanding this complex technology and identifying problems that need to be addressed before products are ready for widespread use.

To my advisors, fellow researchers, family, and friends...

I wouldn't have made it without you.

TABLE OF CONTENTS

ABSTRACT.....	iii
ACKNOWLEDGMENTS	viii
Chapters	
1. INTRODUCTION	1
1.1 References	3
2. LITERATURE REVIEW	5
2.1 Overview	5
2.2 Titanium Dioxide	5
2.3 History and Current Products.....	6
2.4 Previous Laboratory Studies	7
2.5 Field Studies and Modeling	9
2.6 References	11
3. INFLUENCE OF ULTRAVIOLET LIGHT ON PHOTOCATALYTIC TiO ₂ MATERIALS.....	15
3.1 Abstract	15
3.2 Background	16
3.3 Experimental Program	21
3.4 Experimental Results and Discussion	24
3.5 Conclusion	28
3.7 Acknowledgements.....	29
3.8 References	29
4. FABRICATION TECHNIQUES FOR CONCRETE CONTAINING TiO ₂ PHOTOCATALYTIC PARTICLES	36
4.1 Abstract.....	36
4.2 Background.....	37

4.3	Experimental Program	41
4.4	Experimental Results and Discussion	44
4.5	Conclusion	50
4.6	Acknowledgements	51
4.7	References	51
5.	REJUVENATION TECHNIQUES FOR CONCRETE CONTAINING PHOTOCATALYTIC TiO_2 MATERIAL	58
5.1	Abstract	58
5.2	Background	59
5.3	Experimental Program	65
5.4	Experimental Results and Discussion	69
5.5	Conclusion	74
5.6	References	75
6.	PRECAST CONCRETE APPLICATIONS	82
6.1	Abstract	82
6.2	Introduction	82
6.3	Experimental Program	83
6.4	Experimental Results and Discussion	85
6.5	Conclusion	87
7.	CONCLUSIONS AND FUTURE RESEARCH	92
7.1	Conclusions	92
7.2	Future Research	94

ACKNOWLEDGMENTS

The research reported in this dissertation was supported by Advancing Science in America, the Federal Highway Administration, and Unlimited Designs, Inc.

I would like to thank my advisors and mentors, Dr. Paul Tikalsky and Dr. Larry Reaveley, for their support and encouragement, and for the opportunities they provided over the years including nearly 9 years of research.

Further thanks go to Uma Ramasamy and Wade Stinson for their assistance in specimen fabrication, laboratory testing, and general camaraderie. And to Mark Bryant, thank you for your years of advice, service, and knowledge, which kept us safe and productive in the laboratory.

Finally, thank you to my family for their love, support, and motivation to keep working no matter what obstacles I encountered.

CHAPTER 1

INTRODUCTION

The U.S. Environmental Protection Agency's (EPA) National Ambient Air Quality Standard for nitrogen dioxide (NO_2) was changed in 2010, adding a new 1-hour 100 parts per billion (ppb) standard in addition to the previously established 53 ppb annual requirement (U.S., 2012b). Historically, Utah has met the EPA standards for NO_2 (U.S., 2012c). However, the smog inversions experienced in Utah's valleys mainly consist of ozone smog, which is created by a chemical reaction between oxides of nitrogen (NO_x) and volatile organic compounds (U.S., 2012a). Over the past decade, photocatalytic titanium dioxide (TiO_2) has been proven to be able to absorb and oxidize certain harmful pollutants such as NO_x in the presence of ultraviolet (UV) light. It is speculated that each square meter of high-performance photocatalytic material exposed to outdoor sunlight can remove NO_x from 200 cubic meters of air per day (Akbari and Berdahl, 2008).

A few commercial construction products containing TiO_2 are currently available. However, these products focus on bulk materials, instead of products or applications, and their use can increase the cost of the project construction materials by as much as 50% (Civil, 2011). The challenge is to engineer products that are both cost effective and

efficient, while still meeting the needs of the client. The identified areas of research include:

- 1) Determine which types of TiO_2 materials have the highest photocatalytic efficiency.
- 2) Determine methods that reduce the additional cost of adding TiO_2 to a concrete mixture design.
- 3) Determine how surface treatments affect the photocatalytic efficiency of the surface.
- 4) Weather test specimens to identify if any photocatalytic efficiency is lost over time, and if performance is reduced, test for possible rejuvenation methods.
- 5) Determine the influence of UV light intensities, air flow rates, and NO_x pollution concentrations.
- 6) Partner with a local architectural precast company and identify the most practical manufacturing process for utilizing the addition of TiO_2 to their mixture design and identify potential problems.

Chapter 2 provides a literature review containing information on the molecular structure of TiO_2 , the history and current commercially available products, previous laboratory and field studies, and models.

Chapters 3, 4, and 5 are peer reviewed papers which have been published or in the publishing process.

Chapter 3 contains research performed on different TiO_2 types from different manufactures to help identify which crystalline type, particle size, purity, and quantity of TiO_2 would be the most appropriate product to add to the concrete matrix to create a

photocatalytic, NO_x-reducing concrete surface. Chapter 3 also includes the influence of UV light intensities on the photocatalytic efficiency of the surface containing TiO₂, which was then investigated along with the testing of UV light intensities on surfaces at different orientations throughout the day.

Chapter 4 contains testing to identify possible techniques to decrease the quantity of TiO₂ used per square foot of surface area while still maintaining performance by adjusting the thickness of the layer containing TiO₂. It also addresses the effect of finishing techniques to fresh and hardened concrete along with combinations of these techniques. Finally, the influence of curing conditions was considered.

Chapter 5 discusses the effect of weathering the specimens for 120-days. Due to the significant decrease in photocatalytic efficiency, rejuvenation techniques were investigated. Finally, the kinetics of the NO_x reaction including changes in air flow rate and NO_x pollutant concentration were investigated.

Chapter 6 investigates manufacturing techniques from a local architectural precast company. Included are three techniques along with the additional cost associated with adding TiO₂ to their process and any noticeable changes that would be required.

Finally, Chapter 7 contains conclusions generated by the entire research study and suggestions for future research, respectively.

1.1 References

Akbari, H.; Berdahl, P. *Evaluation of Titanium Dioxide as a Photocatalyst for Removing Air Pollutants*. Technical Report for the Public Interest Energy Research Program California Energy Commission: Berkeley, CA, January 2008.

Civil Engineer Group. Paving the Road to Clean Urban Air.

<http://www.civilengineergroup.com/paving-road-clean-urban-air.html> (accessed March 23, 2011).

U.S. Environmental Protection Agency: Basic Information.

<http://www.epa.gov/airquality/ozonepollution/basic.html> (accessed March 26, 2012a).

U.S. Environmental Protection Agency: National Ambient Air Quality Standards

(NAAQS). <http://www.epa.gov/air/criteria.html> (accessed March 26, 2012b).

U.S. Environmental Protection Agency: Nonattainment Status for Each County by Year for Utah. http://www.epa.gov/airquality/greenbook/anay_ut.html (Accessed 26 March 26, 2012c).

CHAPTER 2

LITERATURE REVIEW

2.1 Overview

This literature review will provide a brief summary of TiO_2 's molecular structure, the history and the development of TiO_2 materials, and the current availability of related construction materials. The state of knowledge and practice will be discussed and is broken up into two sections: the findings from laboratory studies, and the field studies and computer modeling. Additional literature reviews are located in Chapters 3, 4, and 5 with more in-depth reviews of the chemical equations governing the NO_x reduction cycle and specific research areas addressed in each chapter.

2.2 Titanium Dioxide

TiO_2 particles naturally crystallize in three forms: rutile, anatase, and brookite. Rutile and anatase have a tetragonal ditetragonal dipyramidal crystal system but have different space group lattices. Brookite has an orthorhombic crystal system that can be transformed into rutile with the application of heat.

Figure 2.1 shows ball and stick models of the different tetragonal lattice systems for rutile, anatase, and brookite (Austin and Lim, 2008; Woodley and Catlow, 2009). It should be noted that the volume for the three lattices are approximately 62, 136, and 257

$\times 10^6 \text{ pm}^3$, respectively. The titanium atoms are light gray and the oxygen atoms are dark gray.

2.3 History and Current Products

TiO₂ powders have been commonly used as white pigments for centuries because they are inexpensive, chemically stable, harmless, and have no absorption in the visible region, leading to their white color (Hashimoto et al., 2005). During the past 30-years, each decade has developed a new use for TiO₂. In the 1980s, powdered TiO₂ began to be used for the photocatalytic production of hydrogen gas (H₂). In the 1990s, photocatalysis and hydrophilic properties of films were produced, and in the 21st century, developments began utilizing TiO₂'s photocatalytic capabilities for the decomposition of pollutants. TiO₂ is photocatalytic, the ability of electrons to move from the valance band to the conduction band allowing for the creation of hydroxyl radicals using light energy, at typical UV irradiation levels at the earth's surface.

Over the past decade, additional commercial cement products have been introduced. One of the largest is *TX Arca*, a cement blend containing TiO₂ produced by Italcementi of Italy. Italcementi is rapidly developing their commercial products with three new US patents granted in the last 2-years (Ancora et al., 2012; Cassar et al., 2011; Cucitore et al., 2011). Italcementi has partnered with Heidelberg Cement, the parent company of Hanson Cement in the United Kingdom, to develop *TioCem*. In a combined effort, they are branding their pollution reducing cements at *TX Active* (Heidelberg, 2012). Another commercial product is *NOxer*, produced by Eurovia in France. *NOxer* is a slurry made of a mineral filler, cement, fibers, and TiO₂, which is manually spread and

used as an overlay (Eurovia, 2009). The final type of product is a surface treatment such as *PURETI*. *PURETI* contains 99% water and 1% TiO_2 , and is applied by an electrostatic spray system that lasts up to 3-years (Pureticlean, 2012).

2.4 Previous Laboratory Studies

There is currently no testing standard for large sample testing. Therefore, testing setups and parameters vary study-to-study. The test setups are commonly based on the International Standard ISO 22197-1 “Fine ceramics (advanced ceramics, advanced technical ceramics) – Test method for air-purification performance of semiconducting photocatalytic materials,” which was adapted from the Japanese Standard JIS TR Z 0018 “Photocatalytic materials – Air purification test procedures.” These tests standards call for using a chemiluminescent NO_x analyzer and an ion chromatograph for analysis of nitrate concentrations (ISO, 2007; JIS, 2002) and are designed to test samples with a surface area of 50 mm by 100 mm.

Previous laboratory testing focuses on the characteristics of the TiO_2 material, characteristics of the concrete material, or the environmental climate. When considering TiO_2 materials choices, anatase is generally considered to have a higher photoactivity than rutile (Blimes, et al. 2000; Hassan et al., 2010). When considering a TiO_2 material to be used for photocatalytics, smaller crystal sizes can cause an increase in photocatalytic oxidation as compared to TiO_2 materials with larger crystal systems (Hashimoto et al., 2000). The materials fineness can also play a role as higher fineness leads to higher photocatalytic oxidation. However, the higher fineness can cause

problems regarding a homogeneous distribution of the powder when the powder is mixed dry with the cement (Husken and Brouwers, 2008).

Increases to total surface area can increase the pollution reduction potential of a construction material as it increases the surface area available to react with pollutants (Hashimoto et al., 2000). Simple methods such as texturing, roughening, or mixture design choices can aid in increasing the total surface area (Poon and Cheung, 2007). Surfaces containing TiO_2 underwent weathered (loaded wheel test) and rotary abrasion. Testing showed that the abraded samples performed similarly to the original samples and the weathered samples actually had a higher NO removal efficiency due to more particles being accessible to the air pollution on the surface layer of the concrete material (Hassan et al., 2012).

Four environmental factors have shown to affect the performance of the photocatalyst: relative humidity (RH), temperature, UV irradiance level, and air flow rates. High relative humidity in the range of 80% is approximately 67% less as effective as compared to 25% RH (Dylla et al., 2010; Yu, 2002). This reaction reduction is due to the role humidity plays in the pollutant adhesion to the materials surface (Beeldens, 2006). As the temperature increases, the NO_x oxidation rate accelerates (Beeldens, 2006). The irradiance requirement to promote the electron from the valence band to the conduction band occurs around $100 \mu\text{W}/\text{cm}^2$. This level of irradiance occurs on the sunny side of a structure even on a cloudy winter day and potentially on most surfaces during a sunny summer day (Kaneko and Okura, 2002). Finally, higher air flows lead to lower NO removal efficiencies; this is due to the decrease in residence time so there is less time for the pollutants to be absorbed by the photocatalytic compound (Dylla et al.,

2010). In summary, the best results were obtained by high temperature ($> 25^{\circ}\text{C}$), low relative humidity, high light intensities, and long contact times. This environment is obtained on hot sunny days in arid climates when the winds are calm. Hot dry days are also when the risk of ozone and smog formation is highest, so the reduction of NO_x concentrations would be most useful in reducing ozone formation (Beeldens, 2006).

Testing on the early age effects of adding TiO_2 to a mixture design as a cement replacement, upwards of 15%, found that the smaller particles of TiO_2 accelerate the hydration reaction more than larger particles. The nucleation effect was more dominant than the cement dilution effect (Jayapalan et al., 2010). Mixtures containing TiO_2 may exhibit decreased fluidity, an increase in water demand, and a decrease time to final set (Nazari and Riahi, 2011).

Zinc oxide (ZnO) is also a photocatalyst but exhibits less vigorous oxidation rates than TiO_2 (Richard et al., 1991), unless under concentrated sunlight (Dindar and Icli, 2001). ZnO has a band gap of 3.37 eV (Ozgur et al., 2005) and the higher band gap energy than TiO_2 requires more energy for the electron to be promoted to the conduction band (Dindar and Icli, 2001). This makes TiO_2 a preferred material for ambient light photocatalyst applications.

2.5 Field Studies and Modeling

In the past few years several large-scale studies have been executed on improving air quality by employing photocatalytic materials in roads, with significant reductions in NO_x levels (Beeldens, 2006). In Antwerp, Belgium, 10,000 m^2 of pavement blocks with a surface layer containing TiO_2 was placed on the parking lanes of a main road. To

measure the quantity of NO_x gases removed from the atmosphere, the bricks were rinsed with water and tested for nitrate (NO₃⁻), concentration that was then used to determine the quantity of NO_x particles removed from the atmosphere. It was found that after 1-year, the air pollution reduction capabilities of the blocks had been reduced by 20%; however, they have not reported the initial or 1-year NO_x reduction rates (Beeldens, 2006) at this time.

The first US highway pavement project using TiO₂ was placed on October 24, 2011 in Missouri in conjunction with a research project at Iowa State University. The 1,500 linear feet two lane road section was a two lift placement that had a 2 inch overlay of Italcementi *TX Active*. Pollution monitoring will be done with meteorological and solar radiation monitors that will be placed on the adjacent sound wall and with an ozone-titration method meter. As part of the study, they will also be testing for changes in road runoff water quality (Cackler et al., 2011). During a 1-year review at the International Concrete Sustainability Conference, held in May 2013, the photocatalytic performance of the specimens was reported to be significantly lower than expected. After 1-year, higher quantities of surface calcium were identified than the calcium levels of the nonweathered laboratory samples (Alleman, 2013).

Another large-scale study found that artificial canyon streets lined with TiO₂ panels saw NO_x reductions of 36.7 to 82% (Maggos et al., 2008).

Determining probable wide-spread pollution reduction is difficult without computer modeling. Taking into account parameters such as 3D geometry, road traffic, effectiveness of pollution control, meteorology, and a surface of *NOxer* pavement, modeling showed that it is probable to have a pollution reduction of 30% at vehicle

heights and an overall NO_x pollution reduction of about 15% at a height of 20 m (Rousseau et al., 2009). Using similar variables, a 2D model created in the Netherlands determined that at 1.5 m a NO_x reduction of 25% may occur (Overman, 2009).

2.6 References

- Alleman, J. The Science and Engineering of Photocatalytic Pavements: Update on 1st US 'TX Active' Highway Application. Presented at International Concrete Sustainability Conference . San Francisco, 2013.
- Ancora, R.; Borsa, M.; Cassar, L. Titanium Dioxide Based Photocatalytic Composites and Derived Products on a Metakaolin Support. US Patent 8,092,586. January 10, 2012.
- Austin, R.; Lim, S. The Sackler Colloquium on Promises and Perils in Nanotechnology for Medicine. *Proceedings of the National Academy of Science* **2008**, *105*, 17217-17221.
- Beeldens, A. *An Environmental Friendly Solution for Air Purification and Self-Cleaning Effect: the Application of TiO₂ as Photocatalyst in Concrete*; Technical Report for Belgian Road Research Centre: Brussels, Belgium, 2006.
- Blimes, S.; Mandelbaum, P.; Alvarez, F.; Victoria, N. Surface and Electronic Structures of Titanium Dioxide Photocatalyst. *Journal of Physical Chemistry B* **2008**, *104*, 9851-9858.
- Cackler, T.; Alleman, J.; Kevern, J.; Sikkema, J. *Environmental Impact Benefits with "TX Active" Concrete Pavement in Missouri DOT Two-Lift Highway Construction Demonstration*; DTFH61-06-H-00011; National Concrete Pavement Technology Center; Ames, IA, 2011.
- Cassar, L.; Cucitore, R.; Pepe, C. Cement-Based Paving Blocks for Photocatalytic Paving for the Abatement of Urban Pollutants. US Patent 7,960,042. June 14, 2011.
- Cucitore, R.; Cangiano, S.; Cassar, L. High Durability Photocatalytic Paving for Reducing Urban Polluting Agents. US Patent 8,039,100. October 18, 2011.
- Dindar, B.; Icli S. Unusual Photoreactivity of Zinc Oxide Irradiated by Concentrated Sunlight. *Journal of Photochemistry and Photobiology A: Chemistry* **2001**, *140*, 263-268.

- Dylla, H.; Hassan, M.; Mohammad, L.; Rupnow, T.; Wright, E. Evaluation of Environmental Effectiveness of Titanium Dioxide Photocatalyst Coating for Concrete Pavement. *Transportation Reserach Record* **2010**, 46-51.
- Eurovia Vinci. NOxer Pavement Treating Pollution at Source. http://www.eurovia.com/media/128787/noxerchausser_a4_gb_bd.pdf (accessed March 26, 2012).
- Hashimoto, K.; Irie, I.; Fujishima, A. TiO₂ Photocatalysis: A Historical Overview and Future Prospects. *Japanese Journal of Applied Physics* **2005**, 44, 8269-8285.
- Hashimoto, K.; Wasada, K.; Toukai, N.; Kominami, H.; Kera, Y. Photocatalytic Oxidation of Nitrogen Monoxide Over Titanium Oxide Nanocryastals Large Size Areas. *Journal of Photochemistry and Photobiology A: Chemistry* **2000**, 136, 103-109.
- Hassan, M.; Dylla, H.; Mohammad, L.; Rupnow, T. *Effect of Application Methods on the Effectiveness of Titanium Dioxide as a Photocatalyst Compound to Concrete Pavement*. Proceedings of the Transportation Reserach Board, Washington, D.C., 2010.
- Hassan, M.; Asadi, S.; Kevern, J.; Rupnow, T. Nitrogen Oxide Reduction and Nitrate Measurements on TiO₂ Photocatalytic Pervious Concrete Pavement. *Construction Research Congress*. West Lafayette, LA, 2012.
- Heidelberg Cement. TioCem Reducing Pollution in the Urban Environment. http://www.heidelbergcement.com/NR/rdonlyres/DCDBC089-B141-4E05-92D2-3D0A79ACFBC6/0/Hanson_TioCem.pdf (accessed March 26, 2012).
- Husken, G.; Brouwers, H. Air Purification by Cementitious Materials: Evaluation of Air Purifying Properties. Proceedings of the International Conference on Construction and Building Technology, Kuala Lumpur, 2008.
- ISO 22197-1, International Standard ISO. "Fine Ceramics (Advanced Ceramics, Advanced Technical Ceramics) - Test Method for Air-Purification Performance of Semiconducting Photocatalytic Materials Part 1: Removal of Nitric Oxide." 2007.
- Jayapalan, A.; Lee, B.; Fredrich, S.; Kurtis, K. Influence of Additions of Anatase TiO₂ Nanoparticles on Early-Age Properties of Cement Based Materials. *Journal of the Transportation Reserach Board* **2010**, 41-46.
- JIS 0018:2002, Japanese Industrial Standards TR Z. "Photocatalytic Materials -- Air Purification Test Procedure." 2002.

- Kaneko, M.; Okura, I. Design, Preparation and Characterization of Highly Active Metal Oxide Photocatalysts. In *Photocatalysis: Science and Technology*, 2003; Springer: New York, 2002; 29-49.
- Maggos, T.; Plassais, A.; Bartzis, J.; Vasilakos, N.; Moussiopoulos, N.; Bonafous, L. Photocatalytic Degradation of NO_x in a Pilot Street Canyon Configuraton using TiO₂- Mortar Panels. *Environmental Monitoring and Assessment* **2008**, *136*, 35-44.
- Nazari, A.; Riahi, S. The Effects of TiO₂ Nanoparticles on Properties of Binary Blended Concrete. *Journal of Composite Materials* **2011**, *45(11)*, 1181-1188.
- Overman, H.T.J. Simulation Model for NO_x Distributions in a Street Canyon with Air Purifying Pavement. Thesis, University of Twente, Enschede, the Netherlands, 2009.
- Ozgur, U.; Alivov, Y.; Liu, C.; Teke, A.; Reshchikov, M. A Comprehensive Review of ZnO Materials and Devices. *Journal of Applied Physics* **2005**, *98*.
- Poon, C.S.; Cheung, E. NO Removal Efficiency of Photocatalytic Paving Blocks Prepared with Recycled Materials. *Construction and Building Materials* **2007**, *21*, 1746-1753.
- Pureticlean-FAQ. http://www.pureti.com/pc_faq.html (accessed March 26, 2012).
- Richard, C.; Boule, P.; Aubry, J. Oxidizing Species Involved in Photocatalytic Transformations on Zinc Oxide. *Journal of Photochemistry and Photobiology A: Chemistry* **1991**, *60*, 235-243.
- Rousseau, P.; Drouadaine, I.; Maze, M. Le Procédé NO_xer: du Développement Aux Mesures de Depollution sur Site. RGRA-Revue Generale des Routes et des Aerodromes **2009**, *876*, 80-85.
- Seinfeld, J.; Pandis, S. *Atmospheric Chemistry and Physics From Air Pollution to Climate Change*; John Wiley & Sons, Inc.: New Jersey, 2006.
- Woodley, S.; Catlow, C. Structure Prediction of Titania Phases: Implementation of Darwinian versus Lamarckian concepts in an Evolutionary Algorithm. *Computational Materials Science* **2009**, *45*, 84-95.
- Yu, J. *Ambient Air Treatment by Titanium Dioxide Based Photocatalyst in Hong Kong*; Technical Report Prepared for the Environmental Protection Department: Hong Kong, 2002.

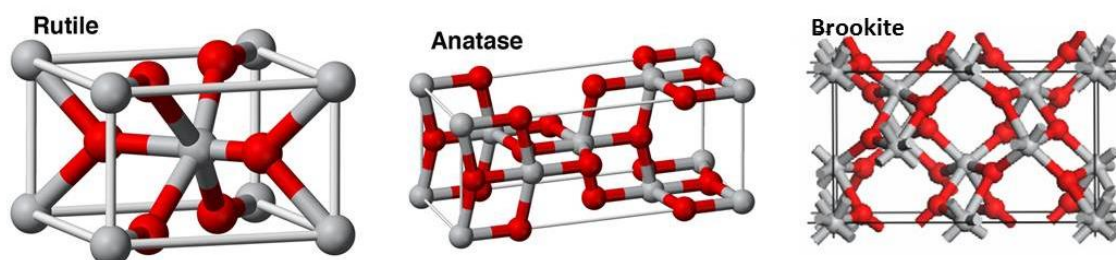


Figure 2.1. Crystal structures of rutile, anatase, and brookite titanium dioxide (Austin and Lim, 2008; Woodley and Catlow, 2009)

CHAPTER 3

INFLUENCE OF ULTRAVIOLET LIGHT ON PHOTOCATALYTIC TiO₂ MATERIALS

3.1 Abstract

NO_x gases affect the diurnal rise and fall of tropospheric ozone. By removing NO_x gases through the use of titanium dioxide (TiO₂) photocatalytic materials, tropospheric ozone concentrations could be reduced. The recent developments related to the photocatalytic pollution reduction capabilities of TiO₂ have led a movement to understand the material properties required to create construction materials that have the potential to reduce NO_x air pollutants. A research program was undertaken to isolate variables that impact the kinetics of TiO₂ reaction. Six TiO₂ materials were tested for NO_x removal efficiencies. The productive TiO₂ materials were then tested at multiple concentrations to determine the effect of ultraviolet (UV) irradiance on their efficiency to reduce NO_x air pollutants. It was found that specific anatase TiO₂ phases manufactured and sized to have high levels of photocatalytic activity could reduce NO_x air pollutants at high efficiencies. The NO_x removal efficiency was 2.4 times higher at a UV irradiance

Reprinted with permission from the American Society of Civil Engineers

Hanson, S.; Tikalsky, P. Influence of Ultraviolet Light on Photocatalytic TiO₂ Materials. *Journal of Materials in Civil Engineering* **2013**, 25 (7), 896-898.

of $1300 \mu\text{W}/\text{cm}^2$ than at $150 \mu\text{W}/\text{cm}^2$, equivalent to a sunny or shady surface, respectively.

3.2 Background

3.2.1 History

Titanium dioxide (TiO_2) powders have been commonly used as white pigments since ancient times because they are inexpensive, chemically stable, benign, and have no absorption in the visible region, leading to their white color (Hashimoto et al., 2005). Over the past 30-years, each decade has developed a new use for TiO_2 .

In the 1970s, a single crystal n-type rutile TiO_2 semiconductor electrode was developed and used to investigate the photoelectrolysis of water. The developed electrode was very stable in solution and could oxidize water to oxygen (Fujishima and Honda, 1972). The “oil crisis” of the 1970s drove the development of using powdered TiO_2 to produce hydrogen gas (H_2) using photocatalytics. However, the generation of H_2 could occur with the use of electrodes, but could not be reproduced with TiO_2 in powdered form. This inconsistency is contributed to the production sites of the H_2 and O_2 gases being located close to each other so that the H_2 and O_2 can recombine back into water before the H_2 can be captured. Organic compounds were added to the system with promising results, but by the mid-1980s, other semiconductors were found to be better suited for future research and development than TiO_2 (Kawai and Sakata, 1980).

In the 1990s, the photocatalytic cleaning, antibacterial, and hydrophilic properties of TiO_2 were investigated. Tiles coated with TiO_2 can remain clean in high exhaust environments due to TiO_2 capabilities of photocatalytic decomposition (Heller, 1995). It

was also found that E-coli would completely disappear from a surface containing TiO_2 after a week of ultraviolet (UV) irradiation (Sunada et al., 1998). The contact angle of water on a TiO_2 containing surface would reach almost 0° when the surface was excited with UV light. This means the surface becomes non-water repellant or highly hydrophilic. The time to decrease the contact angle from 25° to 0° takes approximately 2-hours whereas it takes approximately 1500-hours for the contact angle to return from 0° to 25° , therefore making the TiO_2 hydrophilic properties stable and semipermanent (Wang et al., 1997).

In the 2000s, the technology of using TiO_2 as a photocatalyst to decompose air pollutants began to be studied. The difficulty facing research is this technology is attempting to affect a 3-dimensional space of air pollutants, not just the 2-dimensional surface of the material containing TiO_2 . Large-scale installation of photocatalytic TiO_2 would be required to make a difference in NO_x ($\text{NO} + \text{NO}_2$) pollution concentrations that lead to the development of building materials such as concrete to be a substrate for the TiO_2 particles (Berdahl and Akbari, 2008).

3.2.2 TiO_2 Materials

TiO_2 particles naturally crystallize in three forms: rutile, anatase, and brookite. Rutile is the most common form. It is chemically inert, and can be excited by both visible and UV light (wavelengths smaller than 390 nanometers). The anatase form is only excited by UV light and can be transformed into rutile at high temperatures. Both rutile and anatase have a tetragonal ditetragonal dipyramidal crystal system but have different space group lattices (Austin and Lim, 2008). The volumes of the lattices are

approximately 62 and $136 \times 10^6 \text{ pm}^3$ for rutile and anatase, respectively. The brookite form is not excited by UV light or visible light, but its orthorhombic crystal system can be transformed into rutile with the application of heat.

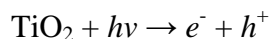
When considering TiO_2 material choices, anatase is generally considered to have a higher photoactivity than rutile (Blimes et al., 2000; Hassan et al., 2010). However, there is evidence that rutile or blending rutile and anatase can be more effective than using anatase alone (Poon and Cheung, 2007). The higher photochemical activity of anatase, as compared to rutile, is believed to be the result of the number of electronic excitation lifetimes being an order of magnitude larger for anatase (Xu et al., 2011).

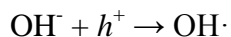
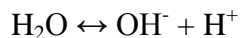
Two processes are used to create TiO_2 . The older sulfate process can produce both anatase and rutile. In this process, ilmenite (FeTiO_3), a weakly magnetic titanium-iron oxide mineral, reacts with sulfuric acid to produce a solution of titanyl sulfate (TiOSO_4). Through thermal hydrolysis, precipitate hydrous titanium dioxide is created. The newer chloride process can only produce rutile TiO_2 due to the high temperatures required during manufacturing. This method begins with crude TiO_2 ore, greater than 90% TiO_2 , which is mixed with carbon and then reacted with chlorine at 900°C to produce titanium tetrachloride (TiCl_4). Using fractional distillation, a high purity TiCl_4 is created which is then oxidized forming TiO_2 and chlorine (Kerr-McGee, 2012; Millennium, 2012).

For both processes, after the creation of the base pigments, chemicals are added to regulate crystal growth, particle size, durability, color stability, and dispersion stability. Particle size control is done with potassium or cesium while surface treatments use alumina, silica, and zirconia. The final step is drying and milling of the particles (Kerr-

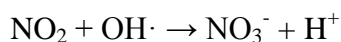
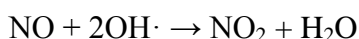
McGee, 2012; Millennium, 2012). The TiO₂ micro- or nano-particles are used as a white pigment in paint, sunscreen, paper, plastics, food coloring, and a number of other applications.

Both rutile and anatase TiO₂ can be an n-type semiconductor photocatalyst (Singh et al., 2010; Warren et al., 2007) with a band energy gap (E_g) for rutile and anatase of 3.0 and 3.2 electron volts (eV), respectively (Kavan et al., 1996). An n-type semiconductor has a filled valance band and an empty conduction band. When subjected to UV light, energy greater than E_g , an electron (e^-) from the valance band is excited to a higher energy state and moves from the valance to the conduction band. When the electron leaves the valance band, a positively charged vacant site, or electron-hole (h^+), remains. The electrons in the conduction band can carry a moderate current, making it a semiconductor (Benedix et al., 2000; Dalton et al., 2002; Daude et al., 1977; Serway and Jewett, 2004). The electron-hole in the valence band provides a site where adsorbed hydroxyl ions (OH^-) and disassociated water (H_2O) can lose an electron, forming a hydroxyl radical (OH^\cdot). Hydroxyl radicals are electrically neutral but highly reactive. The excitation of a valence band electron to the conduction band allowing for the formation of hydroxyl radicals is what makes TiO₂ a catalyst. TiO₂ becomes a photocatalyst because the electron excitation is due to photons ($h\nu$) of UV light. The rate of formation and recombination between a positive hole and a free electron is considered to be very rapid (Hashimoto et al., 2000). Figure 3.1 demonstrates the mechanism of excitation and formation of hydroxyl radicals. The symbolic chemistry for the formation of hydroxyl radicals follows:



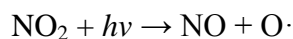


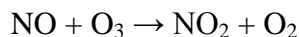
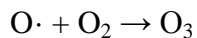
Airborne pollutant molecules can be adsorbed into the TiO_2 particle surface, where they react with the hydroxyl radicals and are oxidized (Berdahl and Akbari, 2008). The nitric oxide (NO) reacts with two hydroxyl radicals, forming one nitrogen dioxide (NO_2) and one water molecule. The nitrogen dioxide can then react with another hydroxyl radical, forming one nitrate (NO_3^-) and a one hydrogen ion. Figure 3.2 is a diagram of the entire process involved with NO_x oxidation. The symbolic chemistry of these reactions follows:



Nitrate is an anion in water and creates a weak nitric acid. The nitrate may need to be washed from the surfaces to free up active sites on the TiO_2 surface. Under practical conditions, reaction products are flushed from the concrete surface by rain (Beeldens, 2006; Husken and Brouwers, 2008), but this may not be the case in arid climates.

NO_x air pollutants are a primary source for oxygen radicals ($\text{O}\cdot$), which leads to one of the most significant means by which ozone is formed and removed from the troposphere. Below are the chemical equations governing ozone formation from NO_x gases.





If the three reactions occur at equal rates, there will be no average change in the levels of any of the constituents throughout a day. However, the generation of O_3 is generally the dominant reaction during the day and the final equation, NO_x titration, is the dominant process during the night. This change in dominance plays a major role in governing the diurnal rise and fall of ozone levels in the troposphere (Nazari and Riahi, 2011; Sillman, 1999).

3.3 Experimental Program

The objective of this experimental program was to evaluate six TiO_2 powdered materials and determine the effect of UV irradiance on the TiO_2 materials photocatalytic efficiency to reduce NO_x air pollutants. These findings were then correlated to UV irradiance exposures of elements in different orientations to help identify their change in potential efficiency due to changes in UV irradiance.

The most commonly used standard on which laboratory tests are based is the International Standard ISO 22197-1 “Fine ceramics (advanced ceramics, advanced technical ceramics) – Test method for air-purification performance of semiconducting photocatalytic materials,” which was adapted from the Japanese Standard JIS TR Z 0018 “Photocatalytic materials – Air purification test procedures.” These tests standards call for using a chemiluminescent NO_x analyzer and an ion chromatograph for analysis of nitrate concentrations (ISO, 2007; JIS, 2002).

3.3.1 *TiO₂ Material Testing System and Procedure*

The photo-reactor system to test laboratory specimens was designed based on a modified International Standard ISO 22197-1. The photo-reactor system contains an air tight stainless steel box with a glass top. The glass top enables UV light from four adjustable black lights to reach the 0.929 m² (1 ft²) specimens located inside the box. An air space of 5 mm (0.20 inch) exists between the bottom of the glass and the top of the specimen. NO_x-contaminated air at 1.0± 0.1 ppm flows into the box, across the top of the specimen, and is exhausted at a flow rate of 8 L/min (0.28 ft³/min). A chemiluminescent NO_x analyzer tests NO_x pollution concentrations from the exhaust line. During testing of the TiO₂ materials, the UV lights were adjusted so an average UV irradiance of 1300 μW/cm² reached the surface of the specimens, the relative humidity was held at 15%, and the temperature was maintained at 25°C. When testing for the effect of UV irradiance on the TiO₂ material's photocatalytic efficiency, the NO_x concentration, air flow, relative humidity, and temperature were held constant. ISO 22197 specifies a UV irradiance of 1000 ± 50 μW/cm². For testing the effect of UV irradiance, the height of the UV lights was adjusted so an average UV irradiance of 1300, 950, 700, 550, 350, and 150 ± 50 μW/cm² reached the sample surface. UV irradiances vary greatly depending on time of year, time of day, and the presence of shadows from clouds or other objects. The maximum of 1300 μW/cm² represents the potential average UV irradiance reaching a sun exposed location on a summer day, whereas 150 μW/cm² represents a potential shadowed location in the spring or fall.

Testing was performed for 2-hours. The first and last 30-minutes, the UV lights were OFF to allow the system to stabilize. At minute 30, the UV lights were turned ON

and the system remained for 60 minutes. The average initial concentration was found using the first and last 30 minutes of the test. An average excited concentration was found by averaging the middle 60 minutes when the UV lights were ON. Photocatalytic efficiency was determined for each specimen using the equation below:

$$\text{Photocatalytic Efficiency (\%)} = \frac{\text{Concentration}_{\text{initial}} - \text{Concentration}_{\text{excited}}}{\text{Concentration}_{\text{initial}}} \times 100$$

3.3.2 Laboratory Samples and Materials

This study began with six different powdered TiO₂ materials, three anatase and three rutile, from three different manufactures. Table 3.1 shows pertinent material properties of the TiO₂ samples supplied by each manufacturers as well as laboratory collected information. Samples A and B are commercially available as photocatalytic grade whereas the other samples are not manufactured for photocatalytic properties and are prepared for other multipurpose applications. TiO₂ powder does not adhere to a hydrating portland cement concrete surface effectively, so to reduce the variables associated with adding the TiO₂ particles into a concrete matrix, plywood specimens were used. The test specimens were made from 1.9 cm (0.75 inch) plywood cut into a 0.929 m² (1 ft²) pieces that were sealed with Teflon to prevent any reaction with the NO_x air pollutants. TiO₂ was then adhered to the plywood surface at concentrations of 32, 11, and 1 g/m². These concentrations represent a potential range of the quantity of particles that would be on the surface and available for photocatalytic reactions if the TiO₂ had been mixed into a concrete matrix.

UV irradiance was found using a digital ultraviolet radiometer, which measures UVA+UVB and has a range from 0 to 1999 $\mu\text{W}/\text{cm}^2$. Field measurements were taken to help estimate the quantity of UV irradiance that reaches different surfaces based on their orientation and surroundings. Measurements were taken every 30 minutes at three locations. All readings were taken on the same day at a height of 0.91 m (3 ft).

3.4 Experimental Results and Discussion

3.4.1 Material Testing

Only two of the six TiO_2 samples, A and B, were found to be highly photocatalytic with photocatalytic efficiencies of 54 and 57% at 1300 $\mu\text{W}/\text{cm}^2$, respectively. Figure 3.3 shows the photocatalytic efficiency data results of test samples with concentrations of 32 g/m^2 . The crystalline lattice phase of anatase is more likely to be photocatalytic than rutile and small particles lead to higher photocatalytic performance (Blimes et al. 2008; Hassan et al., 2010; Husken and Brouwers, 2008). However, TiO_2 material E is high purity anatase and has a relatively low fineness, but still shows a minimal photocatalytic efficiency of only 6%. The three rutile materials, C, D, and F, effectively had 0% photocatalytic efficiency in reducing NO_x pollution. Comparing materials A and B further, while material B has 13% less TiO_2 , it is slightly more efficient at catalyzing NO_x gases. This observation strengthens the need for future study on the influence of particle size and purity on a material's photocatalytic efficiency.

The time required for the NO_x levels to go from initial concentration to excited concentration is rapid, occurring in less than 60 seconds. The excited concentrations remain relatively constant during the testing period when the UV lights are on ON. After

the UV lights are turned OFF, the NO_x pollution concentration returns to initial concentration in approximately 60 seconds. This rapid initial reduction in pollution concentration demonstrates how quickly the TiO₂ is excited by the photons of light that drives this reaction. At the end of the testing cycle, the rapid return to initial concentrations demonstrates the material characteristic is only sustained by UV light. This is unlike the TiO₂ hydrophilic characteristic, which is semipermanent. The NO_x reduction photocatalytic property of TiO₂ requires UV light to reach to surface for the reactions and it is not diminished by initial reactions.

Due to the performance at 32 g/m², testing continued with the specimens that contained A and B TiO₂ materials at 11 and 1 g/m² on the specimen surface. Figure 3.4 shows the changes in efficiencies due to changing the quantity of TiO₂. Specimens with TiO₂ material A had efficiencies of 13, 36, and 54% and material B had efficiencies of 9, 41, and 57% for 1, 11, and 32 g/m², respectively. Overall, the photocatalytic performance of material A and material B are similar without one having a significantly higher photocatalytic efficiency than the other. There is a not a linear relationship through the points for either TiO₂ material, but higher quantities of TiO₂ material produced higher photocatalytic efficiencies. The nonlinearity may be due to the layers of the TiO₂ particles that occurred at 32 g/m² leading to not all TiO₂ particles being available to participate in a reaction. These data show that even with only 1 g/m² of TiO₂ on the surface, a NO_x pollution reduction occurs and the increase in photocatalytic efficiency is rapid from the 1 g/m² to the 11 g/m² specimens.

3.4.2 Irradiance Testing

Testing the UV irradiance's effect on the specimen's photocatalytic efficiency was performed on the 11 and 32 g/m² specimens of both A and B materials. All test specimens showed similar trends. Figure 3.5 shows the effect UV irradiance had on the photocatalytic efficiency of the specimen with 32 g/m² of sample A. The increase in photocatalytic efficiency is near linear between 150 $\mu\text{W}/\text{cm}^2$ to 1300 $\mu\text{W}/\text{cm}^2$ with an R^2 value of 0.97. This linearity is assumed only to continue through the region tested. At what point there is not enough energy to drive the photocatalytic properties of TiO_2 cannot be determined from the data collected during this study. However, having a photocatalytic efficiency of 22% at only 150 $\mu\text{W}/\text{cm}^2$ is promising for practical applications because it means that that NO_x pollution concentration reduction could still occur if photocatalytic TiO_2 was used in shaded applications. For UV irradiances over 1300 $\mu\text{W}/\text{cm}^2$, there may be additional photocatalytic efficiency beyond the 54% found during this study. Irradiance proved to be a dominant variable with specimens showing a photocatalytic efficiency increase of 2.4 times going from 150 $\mu\text{W}/\text{cm}^2$ to 1300 $\mu\text{W}/\text{cm}^2$.

During the spring, summer, and fall, the horizontal surface as well vertical east and west exposures of a structure often reach greater than 1000 $\mu\text{W}/\text{cm}^2$ during the day. A daily cycle of the UV intensities in Salt Lake City, Utah, USA, latitude of 40°47' north, elevation of 1320 m (4330 ft), an arid mountain west location, was recorded on June 7, 2012, a typical summer day, for the different exposures. Readings were limited to 1999 $\mu\text{W}/\text{cm}^2$ due to UV irradiance meter limitations. Figure 3.6 shows the UV irradiation during the day for each orientation. There are well-defined peaks for the east and west exposures during the morning and late afternoon, respectively. The northern

exposure has a low peak of $400 \mu\text{W}/\text{cm}^2$ during the noon hour while the southern exposure has a peak of $650 \mu\text{W}/\text{cm}^2$ around 14:00. As the sun moves farther north or south in the sky during different seasons, it is expected that the northern and southern exposure UV irradiance peaks will be affected. The four cardinal directions had an average UV irradiance during the peak 12 hours of the day of $630 \mu\text{W}/\text{cm}^2$. During these peak hours, the horizontal orientation had an average of $1560 \mu\text{W}/\text{cm}^2$. Therefore, if a specimen containing TiO_2 photocatalyst materials was placed horizontally instead of vertically, considering the differences in UV irradiance only, it could potentially increase its efficiency percentage by 1.7 times based on the equation found in Figure 3.5. There is enough UV irradiance on all surfaces tested to potentially produce some photocatalytic activity even when shaded.

Lin et al. (2008) determined the minimum level of tropospheric ozone in the USA occurs around 6:00 a.m. and the maximum occurs around 3:00 p.m. The maximum concentration levels are 1.5 to 4 times the minimum concentration level depending on location. The similar timing of high UV intensities and ozone levels means that the TiO_2 would be working at its highest efficiency during these peak hours and would be the most effective in reducing NO_x gases and therefore helping to reduce tropospheric ozone. This combination of arid climate and high UV light concentrations in the Mountain West USA create perfect conditions for the anatase TiO_2 tested in this study to reduce the diurnal concentrations of O_3 and NO_x gases.

3.5 Conclusion

The findings in this study demonstrate that some anatase TiO₂ materials have the capability to be photocatalytic and reduce NO_x air pollutants. However, not all anatase forms of TiO₂ are efficient in producing this reduction. This may be a secondary effect of size distribution or related to purity or one of the anatase phases may have been exposed to moisture. The effective anatase phases were approximately 1.0 μm in average size and had purities between 83 and 97%. The ineffective anatase phase had a smaller particle size and greater than 98% purity. The rutile TiO₂ materials did not show any photocatalytic characteristics.

When different quantities of TiO₂ were tested on wood specimens in the photo-reactor system, higher quantities of TiO₂ removed higher quantities of NO_x air pollutants from the air flow. At high quantities, there was a layered effect that is not beneficial as it reduced the percentage of TiO₂ exposed to UV light and NO_x polluted gases.

UV irradiance is a dominating variable when determining the efficiency of a TiO₂ material to reduce NO_x pollutants in air. Higher UV irradiances led to higher efficiencies. Within the testing range, the average efficiency was increased by 240% when the UV irradiance was increased from 150 to 1300 $\mu\text{W}/\text{cm}^2$. This change in efficiency is important when considering possible applications. A typical building façade in Salt Lake City, Utah, USA in June has an average of 630 $\mu\text{W}/\text{cm}^2$ reach its exterior walls during the peak hours of 7 a.m. to 7 p.m. whereas a horizontal surface received an average 1560 $\mu\text{W}/\text{cm}^2$ on the same day over the same time period. Other dominant variables such as temperature, relative humidity, surface application, and air flow rates may also affect a TiO₂ material's photocatalytic efficiency.

A correlation exists between tropospheric ozone generation and NO_x air pollutants. The UV irradiation provided by the sun is strong enough to cause a photocatalytic reaction in TiO₂. If used on a large scale through construction building materials, there is a possibility to reduce the concentration of NO_x pollutants and therefore reduce tropospheric ozone concentrations.

3.7 Acknowledgements

The research was supported in part by the FHWA Dwight David Eisenhower Transportation Fellowship Program and by the Achievement Rewards for College Scientists, Utah Chapter.

3.8 References

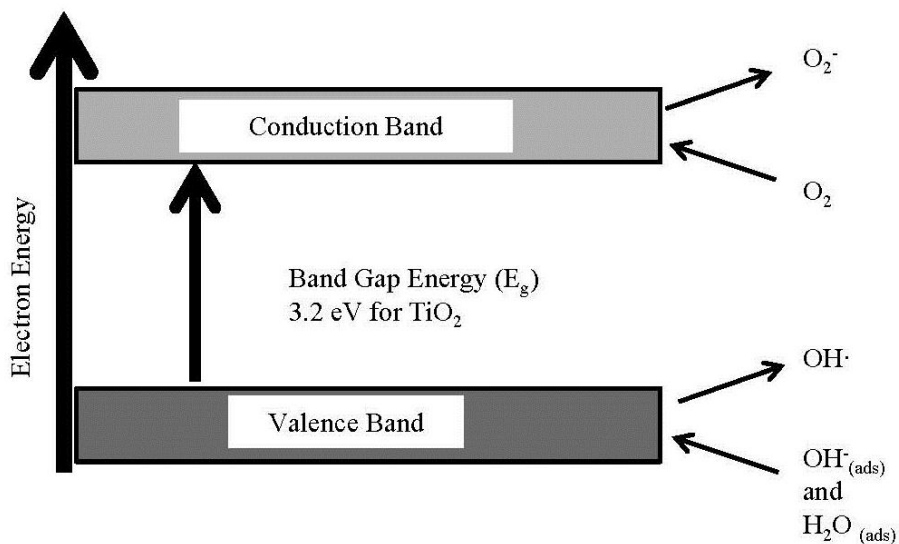
- Austin, R.; Lim, S. The Sackler Colloquium on Promises and Perils in Nanotechnology for Medicine. *Proceedings of the National Academy of Science* **2008**, *105*, 17217-17221.
- Beeldens, A. *An Environmental Friendly Solution for Air Purification and Self-Cleaning Effect: the Application of TiO₂ as Photocatalyst in Concrete*; Technical Report for Belgian Road Research Centre: Brussels, Belgium, 2006.
- Benedix, R.; Dehn, F.; Quaas, J.; Orgass, M. Application of Titanium Dioxide Photocatalysis to Create Self-Cleaning Building Materials. *Lacer* **2000**, *5*, 157-168.
- Berdahl, P.; Akbari, H. *Evaluation of Titanium Dioxide as a Photocatalyst for Removing Air Pollutants*. Technical Report for PIER Energy-Related Environmental Research Program California Energy Commission: Berkeley, CA, 2008.
- Blimes, S.; Mandelbaum, P.; Alvarez, F.; Victoria, N. Surface and Electronic Structures of Titanium Dioxide Photocatalyst. *Journal of Physical Chemistry B* **2008**, *104*, 9851-9858.

- Dalton, J.; Janes, P.; Jones, N.; Nicholson, J.; Hallam, K.; Allen, G. Photocatalytic Oxidation of NO_x Gases Using TiO₂: a Surface Spectroscopic Approach. *Environmental Pollution* **2002**, *120*, 415-422.
- Daude, N.; Gout, C.; Jouanin, C. Electronic Band Structure of Titanium Dioxide. *Physical Review B* **1977**, *15*(6), 3229-3235.
- Fujishima, A.; Honda, K. Electrochemical Photolysis of Water at a Semiconductor Electrode. *Nature* **1972**, *238*, 37-38.
- Hashimoto, K.; Irie, H.; and Fujishima, A. TiO₂ Photocatalysis: A Historical Overview and Future Prospects. *Japanese Journal of Applied Physics* **2005**, *44*(12), 8269-8285.
- Hashimoto, K.; Wasada, K.; Toukai, N.; Kominami, H.; Kera, Y. Photocatalytic Oxidation of Nitrogen Monoxide Over Titanium Oxide Nanocrystals Large Size Areas. *Journal of Photochemistry and Photobiology A: Chemistry* **2000**, *136*, 103-109.
- Hassan, M.; Dylla, H.; Mohammad, L.; Rupnow, T. *Effect of Application Methods on the Effectiveness of Titanium Dioxide as a Photocatalyst Compound to Concrete Pavement*. Proceedings of the Transportation Research Board, Washington, D.C. 2010.
- Heller, A. Chemistry and Applications of Photocatalytic Oxidation of Thin Organic Films. *Accounts of Chemical Research* **1995**, *28*(12), 503-508.
- Husken, G.; Brouwers, H. Air Purification by Cementitious Materials: Evaluation of Air Purifying Properties. Proceedings of the International Conference on Construction and Building Technology, Kuala Lumpur, 2008.
- ISO 22197-1, International Standard ISO. "Fine Ceramics (Advanced Ceramics, Advanced Technical Ceramics) - Test Method for Air-Purification Performance of Semiconducting Photocatalytic Materials Part 1: Removal of Nitric Oxide." 2007.
- JIS 0018:2002, Japanese Industrial Standards TR Z. "Photocatalytic Materials -- Air Purification Test Procedure." 2002.
- Kavan, L.; Gratzel, M.; Gilbert, S.; Klemenz, C.; Scheel, H. Electrochemical and Photoelectrochemical Investigation of Single-Crystal Anatase. *Journal of the American Chemical Society* **1996**, *118*, 6716-6723.
- Kawai, T.; Sakata, T. Conversion of Carbohydrate into Hydrogen Fuel by a Photocatalytic Process. *Nature* **1980**, *286*, 474-476.

- Kerr-McGee Chemical LLC. Tailoring TiO₂ Treatment Chemistry to Achieve Desired Performance Properties. <http://www.pcimag.com/articles/tailoring-tio2-treatment-chemistry-to-achieve-desired-performance-properties> (accessed May 24, 2012).
- Lin, J.; Youn, D.; Liang, X.Z.; Wuebbles, D. Global Model Simulation of Summertime U.S. Ozone Diurnal Cycle. *Atmospheric Environment* **2008**, *42*, 8470-8483.
- Millennium Inorganic Chemicals. Titanium Dioxide Manufacturing Processes. http://www.millenniumchem.com/Products+and+Services/Products+by+Type/Titanium+Dioxide+Paint+and+Coatings/r_TiO2+Fundamentals/Titanium+Dioxide+Manufacturing+Processes_EN.htm (accessed May 25, 2012).
- Nazari, A.; Riahi, S. The Effects of TiO₂ Nanoparticles on Properties of Binary Blended Concrete. *Journal of Composite Materials* **2011**, *45*(11), 1181-1188.
- Poon, C.; Cheung, E. NO Removal Efficiency of Photocatalytic Paving Blocks Prepared with Recycled Materials. *Construction and Building Materials* **2007**, *21*, 1746-1753.
- Serway, R.; Jewett, J. Electrical Conduction in Metals, Insulators, and Semiconductors. In *Physics for Scientists and Engineers with Modern Physics*; Brooks/Cole-Thomson Learning: Belmont, 2004; pp 1420-1424.
- Sillman, S. The Relation Between ozone, NO_x and Hydrocarbons in Urban and Polluted Rural Environments. *Atmospheric Environment* **1999**, 1821-1845.
- Singh, A.; Hanisch, J.; Matias, V.; Ronning, F.; Mara, N.; Pohl, D.; Rellinghaus, B.; Reagor, D. Transforming Insulating Rutile Single Crystal into a Fully Ordered Nanometer-Thin Transparent Semiconductor. *Nanotechnology* **2010**, *21*, 1-5.
- Sunada, K.; Kikuchi, Y.; Hashimoto, K.; Fujishima, A. Bactericidal and Detoxification Effects of TiO₂ Thin Film Photocatalysts. *Environmental Science and Technology* **1998**, *32*(5), 726-726.
- Wang, R.; Hashimoto, K.; Fujishima, A.; Chikuni, M.; Kojima, E.; Kitamura, A.; Shimohigoshi, M.; Watanabe, T. Light-Induced Amphiphilic Surfaces. *Nature* **1997**, *388*, 431-432.
- Warren, D.; Shapira, Y.; Kisch, H.; McQuillan, A. Apparent Semiconductor Type Reversal in Anatase TiO₂ Nanocrystalline Films. *The Journal of Physical Chemistry* **2007**, *111*, 14286-14289.
- Xu, M.; Gao, Y.; Moreno, E.; Kunst, M. Photocatalytic Activity of Bulk TiO₂ Anatase and Rutile Single Crystals Using Infrared Absorption Spectroscopy. *American Physical Society* **2011**, *106*, 1-4.

Table 3.1 Titanium dioxide material information

Research Nomenclature	A	B	C	D	E	F
Producer	I	I	II	II	III	III
Designation	PC 105	PC 500	Ti-Pure R-706	Ti-Pure R-902+	1109LPb	1121
TiO ₂ Type	Anatase	Anatase	Rutile	Rutile	Anatase	Rutile
TiO ₂ (%)	96.5	83.4	93	93	98.5	95
Sulfate (%)	0.3	0.3	-	-	0.15	-
Alumina (%)	-	-	2.5	yes	-	Yes
Silica (%)	-	-	3	yes	-	Yes
Particle Size (μm)	1.0	1.0	0.36	0.405	<45	<45
Measured Mean Particle Size (μm)	1.25	1.9	.62	1.37	0.58	.68

Figure 3.1 TiO₂ valance to conduction band mechanism

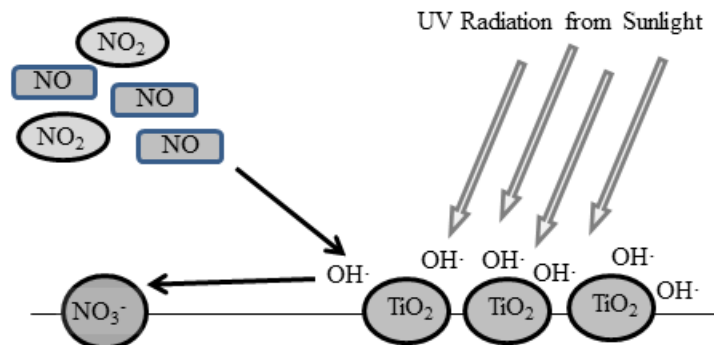


Figure 3.2 NOx oxidation process schematic

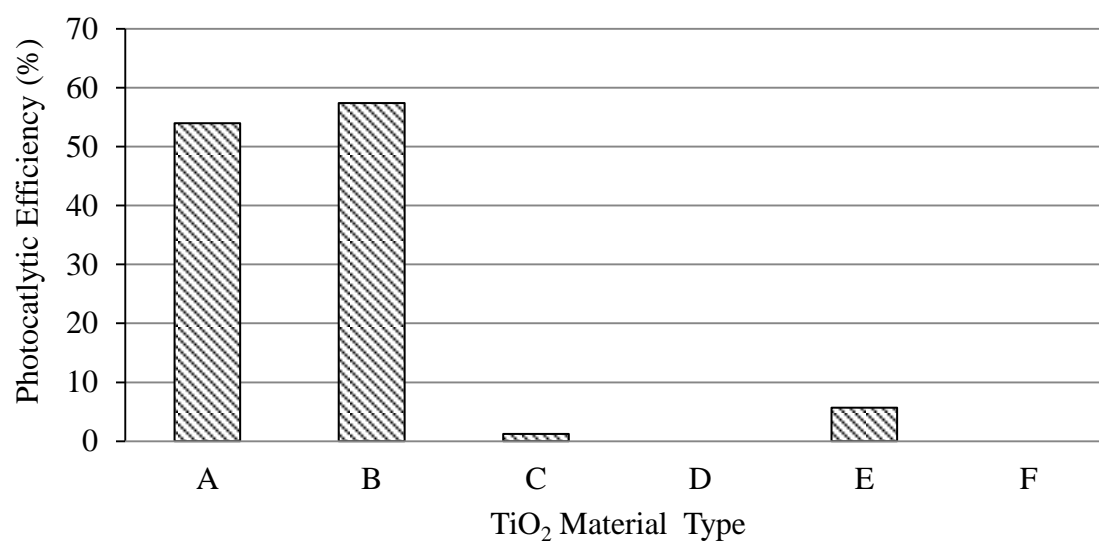


Figure 3.3 NOx air pollutant reduction photocatalytic efficiency of six TiO₂ materials

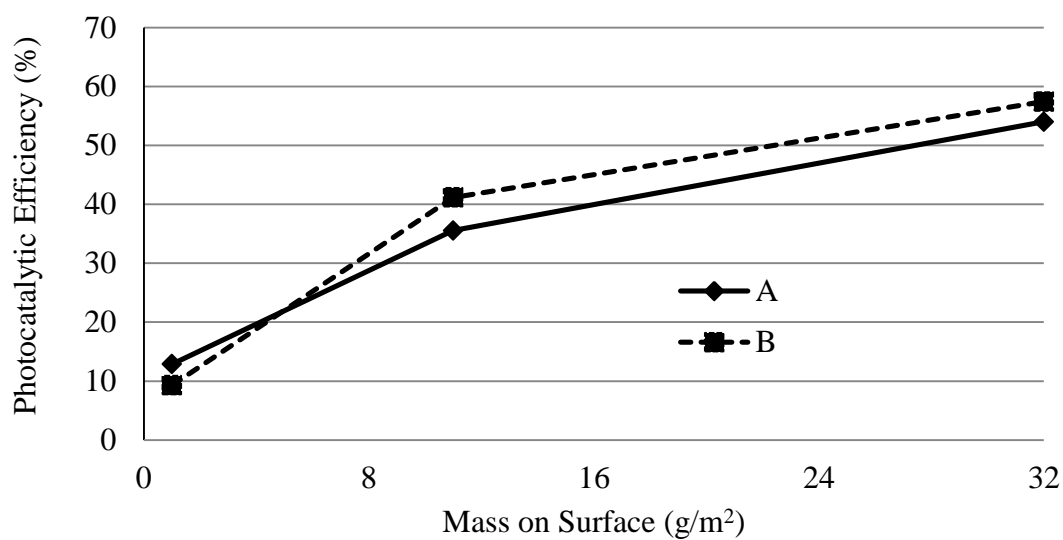


Figure 3.4 Change in efficiency to remove NO_x air pollutants due to carrying quantities of TiO₂ available

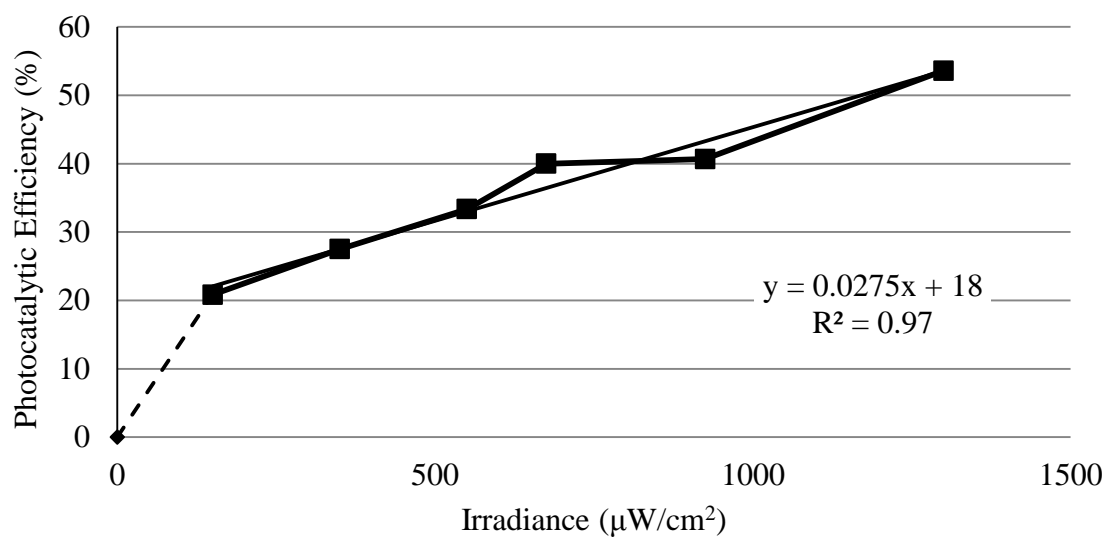


Figure 3.5 Change in photocatalytic efficiency to remove NO_x air pollutants due to varying irradiance on the 32 g/m² of material A specimen

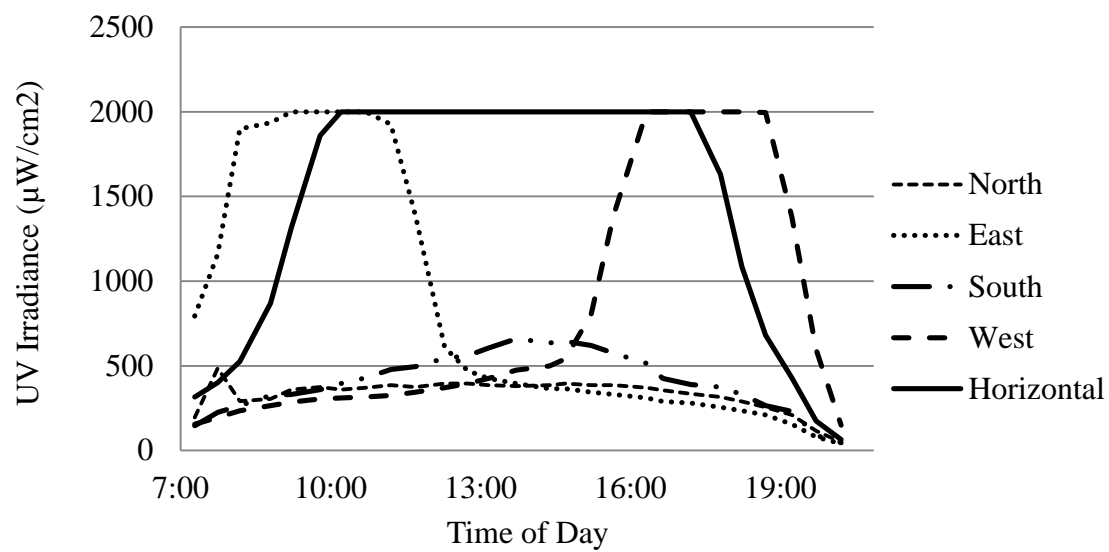


Figure 3.6 UV Irradiance on different orientation exposure throughout the day

CHAPTER 4

FABRICATION TECHNIQUES FOR CONCRETE CONTAINING TiO_2 PHOTOCATALYTIC PARTICLES

4.1 Abstract

The pollution reduction capabilities of photocatalytic titanium dioxide (TiO_2) on tropospheric NO_x gases have recently been developed. Tropospheric NO_x gases affect the diurnal rise and fall of low level ozone. Concrete has shown to be a possible durable media in which photocatalytic TiO_2 can be distributed on a large scale. A research program was undertaken to investigate fabrication techniques to find an efficient and cost-effective method of distributing the TiO_2 onto the surface of the concrete so it can react with NO_x gases in the atmosphere. The effects of curing regiments were also considered. Finally, typical finishing methods such as media blasting, acid etching, and surface tining were addressed to identify their effect on the concretes surface's NO_x reducing efficiency. It was found that the quantity of TiO_2 used in the concrete was not significantly higher when using 15% TiO_2 by cement mass than it was when using 5%

Reprinted with permission from the National Ready Mixed Concrete Association

Hanson, S.; Tikalsky, P. *Fabrication Techniques for Concrete Containing TiO_2* ,
Proceedings from the International Concrete Sustainability Conference, San
Francisco, CA, May 6-8, 2013.

TiO₂. Another cost-saving element was determining the thickness of the layer which contained TiO₂ that would still provide similar NO_x reduction efficiencies as when TiO₂ was used throughout the concrete. Using TiO₂ in a thin top layer had similar NO_x removal efficiency as the specimens that contained TiO₂; however, when vibration was used as the compaction method, there was a decrease in removal efficiency. This decrease was not seen when the TiO₂ was distributed through the specimen. The most efficient and cost-effective method tested was creating a specimen with a thin top coat of TiO₂ that was not mixed into the concrete matrix. Curing conditions showed to have a large effect on NO_x removal efficiency. When the specimens were improperly cured, the crystalline structure did not form completely and the specimens had higher NO_x removal efficiencies than specimens with highly defined crystalline structures. When abrasive finishes were used such as media blasting or sanding, there was a reduction in NO_x removal efficiency. The testing included in this research program determined fabrication methods that apply new concrete technologies to create a cost-effective and an environmentally beneficial concrete.

4.2 Background

4.2.1 History

Titanium dioxide (TiO₂) powders have been commonly used as white pigments since ancient times because they are inexpensive, chemically stable, benign, and have no absorption in the visible region, leading to their white color (Hashimoto et al., 2005). Over the past 40-years, each decade has developed a new use for TiO₂.

In the 1970s, a single crystal n-type rutile TiO_2 semiconductor electrode was developed and used to investigate the photo electrolysis of water. The developed electrode was very stable in solution and could oxidize water to oxygen (Fujishima and Honda, 1972). The “oil crisis” of the 1970s drove the development of using powdered TiO_2 to produce hydrogen gas (H_2) using photocatalytics. However, the generation of H_2 could occur with the use of electrodes, but could not be reproduced with TiO_2 in powdered form. By the mid-1980s, other semiconductors were found to be better suited for future research and development than TiO_2 (Kawai and Sakata, 1980).

In the 1990s, the photocatalytic cleaning, antibacterial, and hydrophilic properties of TiO_2 were investigated. Tiles coated with TiO_2 can remain clean in high exhaust environments due to TiO_2 capabilities of photocatalytic decomposition (Heller, 1995). It was also found that E-coli would completely disappear from a surface containing TiO_2 after a week of ultraviolet (UV) irradiation (Sunada et al., 1998). The contact angle of water on a TiO_2 -containing surface would reach almost 0° when the surface was excited with UV light. The TiO_2 's hydrophilic properties are stable and semipermanent (Wang et al., 1997).

In the 2000s, the technology of using TiO_2 as a photocatalyst to decompose air pollutants began to be studied. The difficulty facing research is the technology is attempting to affect a 3-dimensional space of air pollutants, not just the 2-dimensional surface of the material containing TiO_2 . Large-scale installation of photocatalytic TiO_2 would be required to make a difference in NO_x ($=\text{NO} + \text{NO}_2$) pollution concentrations that lead to the development of building materials such as concrete to be a substrate for the TiO_2 particles (Berdahl and Akbari, 2008).

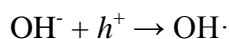
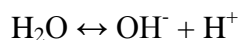
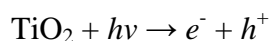
4.2.2 TiO_2 Materials

TiO_2 particles naturally crystallize in three forms: rutile, anatase, and brookite. Rutile is the most common form. It is chemically inert, and can be excited by both visible and UV light (wavelengths smaller than 390 nanometers). The anatase form is only excited by UV light and can be transformed into rutile at high temperatures (Austin and Lim, 2008). The brookite form is not excited by UV light or visible light but it can be transformed into rutile with the application of heat.

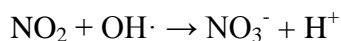
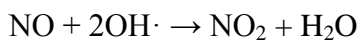
When considering TiO_2 material choices, anatase is generally considered to have a higher photoactivity than rutile (Blimes et al., 2000; Hassan et al., 2010). However, there is evidence that rutile or blending rutile and anatase can be more effective than using anatase alone (Poon and Cheung, 2007). The higher photochemical activity of anatase, as compared to rutile, is believed to be the result of the number of electronic excitation lifetimes being an order of magnitude larger for anatase (Xu et al., 2011).

Rutile and anatase TiO_2 both can be an n-type semiconductor photocatalyst (Singh et al., 2010; Warren et al., 2007) with a band energy gap (E_g) for rutile and anatase of 3.0 and 3.2 electron volts (eV), respectively (Kavan et al., 1996). An n-type semiconductor has a filled valance band and an empty conduction band. When subjected to UV light, energy greater than E_g , an electron (e^-) from the valance band is excited to a higher energy state and moves from the valance to the conduction band. When the electron leaves the valance band, a positively charged vacant site, or electron-hole (h^+), remains. The electrons in the conduction band can carry a moderate current, making it a semiconductor (Benedix et al., 2000; Dalton et al., 2002; Daude et al., 1977; Serway and Jewett, 2004). The electron-hole in the valence band provides a site where adsorbed

hydroxyl ions (OH^-) and disassociated water (H_2O) can lose an electron forming a hydroxyl radical ($\text{OH}\cdot$). Hydroxyl radicals are electrically neutral but highly reactive. The excitation of a valence band electron to the conduction band allowing for the formation of hydroxyl radicals is what makes TiO_2 a catalyst. TiO_2 becomes a photocatalyst because the electron excitation is due to photons ($h\nu$) of UV light. The rate of formation and recombination between a positive hole and a free electron is considered to be very rapid (Hashimoto et al., 2000). The symbolic chemistry for the formation of hydroxyl radicals follows:



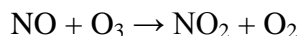
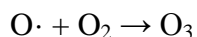
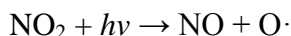
Airborne pollutant molecules can be adsorbed into the TiO_2 particle surface, where they react with the hydroxyl radicals and are oxidized (Berdahl and Akbari, 2008). The nitric oxide (NO) reacts with two hydroxyl radicals, forming one nitrogen dioxide (NO_2) and one water molecule. The nitrogen dioxide can then react with another hydroxyl radical, forming one nitrate (NO_3^-) and a one hydrogen ion. The symbolic chemistry of these reactions follows:



Nitrate is an anion in water and creates a weak nitric acid. The nitrate may need to be washed from the surfaces to free up active sites on the TiO_2 surface. Under

practical conditions, reaction products are flushed from the concrete surface by rain (Beeldens, 2006; Husken and Brouwers, 2008), but this may not be the case in arid climates.

NO_x air pollutants are a primary source for oxygen radicals (O·), which leads to one of the most significant means by which ozone is formed and removed from the troposphere. Below are the chemical equations governing ozone formation from NO_x gases.



If the three reactions occur at equal rates, there will be no average change in the levels of any of the constituents throughout a day. However, the generation of O₃ is generally the dominate reaction during the day and the final equation, NO_x titration, is the dominate process during the night. This change in dominance plays a major role in governing the diurnal rise and fall of ozone levels in the troposphere (Nazari and Riahi, 2011; Sillman, 1999).

4.3 Experimental Program

The objective of this experimental program was to investigate possible fabrication techniques that utilize photocatalytic TiO₂ in a concrete matrix. Photocatalytic grade TiO₂ is an expensive material, approximately \$3,000 per 100 kg, so using the least amount possible per surface square meter, with the greatest performance in reducing NO_x

pollution, would be the most economically and environmentally favorable option for this new technology to be used on a large scale. Many of techniques tested mimic the precast industry methods as they often use multiple lifts and finishing techniques.

4.3.1 Materials and Methods

Typical construction materials were used for the production of test specimens. ASTM C150 Type I, Type II/V, Type III, and White Type I/II portland cements were used along with ASTM C33 fine aggregate concrete sand, which had a fineness modulus and absorption of 2.90 and 1.9%, respectively. The mortar was mixed following the procedures of ASTM C109 with a constant water-cement ratio of 0.485. If variables tested during this investigation required special procedures, they are specified at the beginning of the appropriate section. The control specimens were made with Type II/V cement, contained 5% TiO_2 by cement mass in only a $\frac{1}{4}$ of the specimen thickness, were not vibrated, had a steel trowel finish, and were cured according to ASTM C192. All test specimens were 0.929 m^2 (1 ft^2) by 1.9 cm (0.75 inch) thick.

The photocatalytic TiO_2 used for this project is 96.5% TiO_2 with a mean particle size of $1.0 \text{ }\mu\text{m}$. The TiO_2 is considered an aggregate and the amount used in the mixtures is based on a mass percentage of cement.

4.3.2 Testing System and Procedure

The photo-reactor system developed to test laboratory specimens was designed based on a modified International Standard ISO 22197-1 “Fine ceramics (advanced ceramics, advanced technical ceramics) – Test method for air-purification performance of

semiconducting photocatalytic materials,” which was adapted from the Japanese Standard JIS TR Z 0018 “Photocatalytic materials – Air purification test procedures.” These tests standards call for using a chemiluminescent NO_x analyzer and an ion chromatograph for analysis of nitrate concentrations (ISO, 2007; JIS, 2002). The photo-reactor system contains an air tight stainless steel box with a glass top. The glass top enables UV light from four adjustable black lights to reach the specimens located inside the box. An air space of 5 mm (0.20 inch) exists between the bottom of the glass and the top of the specimen. NO_x contaminated air at 1.0± 0.1 ppm flows into the box, across the top of the specimen, and is exhausted at a flow rate of 8 L/min. A chemiluminescent NO_x analyzer tests NO_x pollution concentrations from the exhaust line. During testing of the specimens, UV lights were adjusted so an average UV irradiance of 1300 μW/cm² reached the surface of the specimens. The relative humidity was held at 15% and the temperature was maintained at 25°C.

Testing was performed for 2-hours. The first and last 30-minutes, the UV lights were OFF to allow the system to stabilize and provide an initial NO_x concentration. At minute 30, the UV lights were turned ON and the system remained for 60 minutes. During this 60 minutes, an excited concentration was determined. Photocatalytic efficiency was determined for each specimen using the equation below:

$$\text{Photocatalytic Efficiency (\%)} = \frac{\text{Concentration}_{\text{initial}} - \text{Concentration}_{\text{excited}}}{\text{Concentration}_{\text{initial}}} \times 100$$

4.4 Experimental Results and Discussion

4.4.1 Types of Cement

Four cements were tested to determine if cement type would affect the photocatalytic efficiency. Cements tested included gray Type I, Type II/V, Type III, and a White Type I/II. All of the gray cements performed similarly; however, the Type I cement had the lightest color and had the highest photocatalytic efficiency of the gray cements. The white cement had a higher photocatalytic efficiency than all of the gray cements. These results suggest that the color of the cement has more effect on the photocatalytic efficiency of a specimen than the type of cement. It is not realistic to match a shade of cement to a type of cement as the color of a type of cement varies from cement plant to cement plant and even batch to batch.

4.4.2 Quantity of TiO_2

The quantity of TiO_2 used per square foot of surface area is an important factor due to the additional cost associated with adding TiO_2 to the mixture design. A range from 3 to 15% TiO_2 was added to the mixture design. The mixture with 3% TiO_2 had a photocatalytic efficiency of 9% whereas the specimen containing 15% TiO_2 had an efficiency of 19%. The increase in photocatalytic efficiency was not linear, and specimens with 5% and greater TiO_2 percentages had similar results. This plateau effect is likely caused by the layering of particles, which reduces the total number of TiO_2 particles available to participate in the photo-catalytic reactions.

Using the given cost of TiO_2 as \$3,000 per 100 kg, the specimen containing 5% TiO_2 has a material cost \$0.75 higher than an equivalent specimen with no TiO_2 . The additional cost of adding 5% TiO_2 to this mortar mixture design is \$424 per cubic meter.

The addition of high percentages of TiO_2 caused the mortar paste to become sticky due to the small particle size of the TiO_2 , similar to the effect of adding silica fume to mortar. This would require the additional cost of adding higher dosages of super-plasticizers or water reducers to have the same mixture workability.

4.4.3 Layer Thickness

Two methods were used to test the effect of reducing the quantity of TiO_2 required per surface area. The first was to mix the TiO_2 into only a quarter of the specimen. A quarter thickness of the specimen was chosen due to the ability to still easily ensure full coverage of the surface with mortar containing TiO_2 . Second, lightly adhesive paper was coated with TiO_2 then placed TiO_2 side up in the form. Mortar containing no TiO_2 was then cast over the adhesive paper. After de-molding the specimens at 24-hours, the specimens were rinsed off with water to remove any loose TiO_2 particles.

For a TiO_2 particle to be active in the photoreaction process and oxidize the NO_x pollutants, the TiO_2 particle must both receive energy from sunlight and be able to come into contact with the NO_x pollutants. For this to happen, the TiO_2 particles need to be at the surface of the mortar specimen and not covered with cement. When this is considered, there is the potential for large cost savings by using the TiO_2 in only a portion of the specimen depth. Figure 4.1 shows the effect of four specimens types tested.

The specimens that had a thin top coat of TiO_2 had a photocatalytic efficiency of 74%, which is more than 3.5 times more effective as the specimens that had TiO_2 throughout. The procedure for applying TiO_2 as a top coat does require extra sample preparation time to adhere the TiO_2 to the lightly adhesive paper; however, it saves cost by using a minimal amount of TiO_2 and does not require additional admixtures. One major deterrent from this method is that the TiO_2 , while securely attached to the concrete, is visible. Practical applications would limit its use to situations when white cement is being used, or when the desired surface has a marbled effect to it. Figure 4.2 shows what the surface of this highly effective method would look like with a grey portland cement specimens.

If the TiO_2 is to be mixed into the concrete, there are two options available. First is to add TiO_2 throughout the specimen. This method has a lower photocatalytic efficiency than using a thin top coat, uses a much higher quantity of TiO_2 , and requires more admixtures to maintain workability, both of which adds extra cost. However, the only additional procedural steps are measuring and adding TiO_2 powder.

If the specimens are not to be vibrated, a good alternative would be to use a multi-lift procedure where only the lift that will be exposed to the atmosphere contains TiO_2 particles. The specimens that were poured in two lifts with only the top quarter of the specimen containing TiO_2 did not have a significant reduction in photocatalytic efficiency as compared to the specimen with TiO_2 throughout. This refers back to the basic chemistry kinetics that only the surface TiO_2 particles can participate in the photocatalytic reactions and oxidize the NO_x pollutants. Therefore, the thickness of the layer containing TiO_2 does not control the photocatalytic efficiency of the surface.

However, when specimens with only the top lift containing TiO₂ were vibrated, there was a reduction of photocatalytic efficiency because of a dilution effect caused by the mixing of the layer containing TiO₂ and the layer that did not contain TiO₂.

4.4.4 Curing Conditions

Different curing conditions caused differences in the development of the crystalline structure of the concrete surface. Using a scanning electron microscope (SEM) and backscattered electrons (BSE), the surfaces of the specimens were imaged. When using BSE, the brighter areas represent areas that contain heavier elements. The two extreme conditions included hot/dry, which consisted of 38 ± 2 °C (95 ± 10 °F) and 35% relative humidity, and ASTM C192 standards, which consists of 23 ± 2 °C (73.5 ± 3.5 °F) and 100% relative humidity, and are shown in Figure 4.3 at 5,000 magnifications. Part A of Figure 4.3 shows a surface that is low is crystalline structure and a surface filled with voids, the dark locations on the image. Part B of the Figure 4.3 shows the highly crystalline structure created when the specimens were cured according to ASTM C192 standards.

The specimens cured in the hot and dry conditions had an average photocatalytic efficiency 60% higher than the ASTM cured specimens. This increase in photocatalytic efficiency is expected to be due to the increased quantity of TiO₂ particle that can be subjected to UV irradiation and pollutants due to the gaps in the crystalline structure at the surface of the specimens. The highly crystalline structure may also be completely covering more of the TiO₂ particles that would lead to a reduction in photocatalytic efficiency.

4.4.5 Fresh Concrete Finishing Methods

The finishing method of the fresh concrete generally did not impact the specimens' photocatalytic efficiency. Figure 4.4 shows the photocatalytic efficiency of five finishing methods tested. The magnesium trowel was the only method tested that did have a significant reduction in photocatalytic efficiency. One unexpected result was the specimens that were tinned did not have a significant increase in photocatalytic efficiency. This result was unexpected because the total surface area of the tinned specimens is nearly double the surface area of the smooth specimens. Figure 4.5 shows one of the tinned specimens. The similar photocatalytic efficiency results of the tinned specimens as the other specimens is contributed to the UV light only reaching a portion of the surface due to the shadows caused by the tinning.

4.4.6 Hardened Concrete Finishing Methods and Colored Concrete

Finishing methods are commonly used in the precast industry to affect the aesthetics of the products. Typical finishes include media blasting, sanding, and acid etching. Figure 4.6 shows the effect these finishing methods and coloring had on similar concrete specimens with 5% TiO_2 in the top quarter of the specimens. Media blasting had the most prevalent effect in reducing the photocatalytic efficiency of the specimen with an average photocatalytic efficiency of only 4.5% compared to the control specimen of 17%. Specimens that were sanded also experienced a substantial reduction in photocatalytic efficiency. It is expected that both the media blasted and sanded specimens experienced the reduction in photocatalytic efficiency due to the weak bond between the hydrated cement and TiO_2 particles. TiO_2 particles are being removed from

the surface during these finishing methods. Figure 4.7 shows an energy dispersive x-ray spectroscopy (EDS) map of the surface of the specimens at 15,000 times magnification. Each dot is a point where TiO_2 was detected. The dense areas of dots are locations where TiO_2 particles exist. Part A of Figure 4.7 is of the control specimen; there are multiple areas of high density dots, which have been circled. Part B is the EDS map of the sanded specimen and similar results were found for the corn cob media blast specimen. There are no areas of high density, which means in this area, there were no TiO_2 particles on the surface.

Acid etching did not reduce the photocatalytic efficiency of the specimens as much as media blasting or sanding, but it did cause a reduction. Acid etching dissolves the cement and the boundary layer between the cement and the TiO_2 particles is a vulnerable location in the concrete matrix. This would reduce the total quantity of TiO_2 on the surface of the specimen and therefore reduce the specimen's photocatalytic efficiency.

The addition of powered concrete color proved to also reduce the specimen's photocatalytic efficiency. Both red and grey powder colors were used and had similar results. It is believed that the reduction in efficiency is due to the darker color of the specimen, which does not reflect sunlight as well as the lighter noncolored specimens. This would reduce the amount of UV irradiation available for the photocatalytic reaction and therefore reduce the efficiency.

4.4.7 Combination Effect

A series of specimens were made with a combination of variables from the above mentioned categories. Figure 4.8 shows the range of possible photocatalytic efficiencies when using TiO_2 mixed into the specimens and cured according to ASTM C192 standards. By using combinations of cement type, percentage of TiO_2 , and finishing methods, expected photocatalytic efficiency can be observed and quantified. Options to increase photocatalytic efficiency include using white cement, increasing the percentage of TiO_2 , and having a slightly textured finish. Choosing options that increase the photocatalytic efficiency could be used to offset finishing methods such as color or media blasting that reduce the photocatalytic efficiency. The most photocatalytic efficient mixture design used white cement with high quantities of TiO_2 and had no surface treatments. The least photocatalytic efficient mixture used gray cement, low levels of TiO_2 , and was colored.

4.5 Conclusion

The findings in this study demonstrate that a wide range of photocatalytic efficiencies are possible when using concrete or mortar as a substrate to contain TiO_2 particles. 5% TiO_2 by cement mass may provide a good balance between performance and cost; however, 10% was the greater efficiency. By using a lift procedure, the thickness of the layer containing TiO_2 could be reduced and therefore could reduce cost further without sacrificing photocatalytic efficiency. However, using vibration for compaction could impact the performance of the specimen if the TiO_2 is only in a portion of the thickness of the specimen. The most efficient and cost-effective method tested was

achieved by creating a thin top coat of TiO_2 on the specimen surface which was not mixed into the concrete matrix. Curing conditions had a large effect on photocatalytic efficiency as specimens cured to ASTM C192 standards were significantly less efficient than specimens cured in a higher temperature/lower relative humidity environment. Media blasting, sanding, and acid etching dislodged the TiO_2 particles on the specimen surface, reducing the specimen's photocatalytic efficiency.

This research study tested methods and procedures often used in the precast concrete industry and incorporated the addition of photocatalytic TiO_2 particles. The findings of this study will help to create an efficient and cost-effective option to help reduce the NO_x pollutants in the atmosphere.

4.6 Acknowledgements

The research was supported in part by the FHWA Dwight David Eisenhower Transportation Fellowship Program and by the Achievement Rewards for College Scientists, Utah Chapter.

4.7 References

- Austin, R.; Lim, S. The Sackler Colloquium on Pormoses and Perils in Nanotechnology for Medicine. *Proceedings of the National Academy of Science* **2008**, *105*, 17217-17221.
- Beeldens, A. *An Environmental Friendly Solution for Air Purification and Self-Cleaning Effect: the Application of TiO_2 as Photocatalyst in Concrete*; Technical Report for Belgian Road Research Centre: Brussels, Belgium, 2006.
- Benedix, R.; Dehn, F.; Quaas, J.; Orgass, M. Application of Titanium Dioxide Photocatalysis to Create Self-Cleaning Building Materials. *Lacer* **2000**, *5*, 157-168.

- Berdahl, P.; Akbari, H. *Evaluation of Titanium Dioxide as a Photocatalyst for Removing Air Pollutants*. Technical Report for PIER Energy-Related Environmental Research Program California Energy Commission: Berkeley, CA, 2008.
- Blimes, S.; Mandelbaum, P.; Alvarez, F.; Victoria, N. Surface and Electronic Structures of Titanium Dioxide Photocatalyst. *Journal of Physical Chemistry B* **2008**, *104*, 9851-9858.
- Dalton, J.; Janes, P.; Jones, N.; Nicholson, J.; Hallam, K.; Allen, G. Photocatalytic Oxidation of NO_x Gases Using TiO₂: a Surface Spectroscopic Approach. *Environmental Pollution* **2002**, *120*, 415-422.
- Daude, N.; Gout, C.; Jouanin, C. Electronic Band Structure of Titanium Dioxide. *Physical Review B* **1977**, *15*(6), 3229-3235.
- Fujishima, A.; Honda, K. Electrochemical Photolysis of Water at a Semiconductor Electrode. *Nature* **1972**, *238*, 37-38.
- Hashimoto, K.; Irie, H.; and Fujishima, A. TiO₂ Photocatalysis: A Historical Overview and Future Prospects. *Japanese Journal of Applied Physics* **2005**, *44*(12), 8269-8285.
- Hashimoto, K.; Wasada, K.; Toukai, N.; Kominami, H.; Kera, Y. Photocatalytic Oxidation of Nitrogen Monoxide Over Titanium Oxide Nanocrystals Large Size Areas. *Journal of Photochemistry and Photobiology A: Chemistry* **2000**, *136*, 103-109.
- Hassan, M.; Dylla, H.; Mohammad, L.; Rupnow, T. *Effect of Application Methods on the Effectiveness of Titanium Dioxide as a Photocatalyst Compound to Concrete Pavement*. Proceedings of the Transportation Research Board, Washington, D.C. 2010.
- Heller, A. Chemistry and Applications of Photocatalytic Oxidation of Thin Organic Films. *Accounts of Chemical Research* **1995**, *28*(12), 503-508.
- Husken, G.; Brouwers, H. Air Purification by Cementitious Materials: Evaluation of Air Purifying Properties. Proceedings of the International Conference on Construction and Building Technology, Kuala Lumpur, 2008.
- ISO 22197-1, International Standard ISO. "Fine Ceramics (Advanced Ceramics, Advanced Technical Ceramics) - Test Method for Air-Purification Performance of Semiconducting Photocatalytic Materials Part 1: Removal of Nitric Oxide." 2007.
- JIS 0018:2002, Japanese Industrial Standards TR Z. "Photocatalytic Materials -- Air Purification Test Procedure ." 2002.

- Kavan, L.; Gratzel, M.; Gilbert, S.; Klemenz, C.; Scheel, H. Electrochemical and Photoelectrochemical Investigation of Single-Crystal Anatase. *Journal of the American Chemical Society* **1996**, *118*, 6716-6723.
- Kawai, T.; Sakata, T. Conversion of Carbohydrate into Hydrogen Fuel by a Photocatalytic Process. *Nature* **1980**, *286*, 474-476.
- Nazari, A.; Riahi, S. The Effects of TiO₂ Nanoparticles on Properties of Binary Blended Concrete. *Journal of Composite Materials* **2011**, *45(11)*, 1181-1188.
- Poon, C.; Cheung, E. NO Removal Efficiency of Photocatalytic Paving Blocks Prepared with Recycled Materials. *Construction and Building Materials* **2007**, *21*, 1746-1753.
- Serway, R.; Jewett, J. Electrical Conduction in Metals, Insulators, and Semiconductors. In *Physics for Scientists and Engineers with Modern Physics*; Brooks/Cole-Thomson Learning: Belmont, 2004; pp 1420-1424.
- Sillman, S. The Relation Between Ozone, NO_x and Hydrocarbons in Urban and Polluted Rural Environments. *Atmospheric Environment* **1999**, 1821-1845.
- Singh, A.; Hanisch, J.; Matias, V.; Ronning, F.; Mara, N.; Pohl, D.; Rellinghaus, B.; Reagor, D. Transforming Insulating Rutile Single Crystal into a Fully Ordered Nanometer-Thin Transparent Semiconductor. *Nanotechnology* **2010**, *21*, 1-5.
- Sunada, K.; Kikuchi, Y.; Hashimoto, K.; Fujishima, A. Bactericidal and Detoxification Effects of TiO₂ Thin Film Photocatalysts. *Environmental Science and Technology* **1998**, *32(5)*, 726-726.
- Wang, R.; Hashimoto, K.; Fujishima, A.; Chikuni, M.; Kojima, E.; Kitamura, A.; Shimohigoshi, M.; Watanabe, T. Light-Induced Amphiphilic Surfaces. *Nature* **1997**, *388*, 431-432.
- Warren, D.; Shapira, Y.; Kisch, H.; McQuillan, A. Apparent Semiconductor Type Reversal in Anatase TiO₂ Nanocrystalline Films. *The Journal of Physical Chemistry* **2007**, *111*, 14286-14289.
- Xu, M.; Gao, Y.; Moreno, E.; Kunst, M. Photocatalytic Activity of Bulk TiO₂ Anatase and Rutile Single Crystals using Infrared Absorption Spectroscopy. *American Physical Society* **2011**, *106*, 1-4.

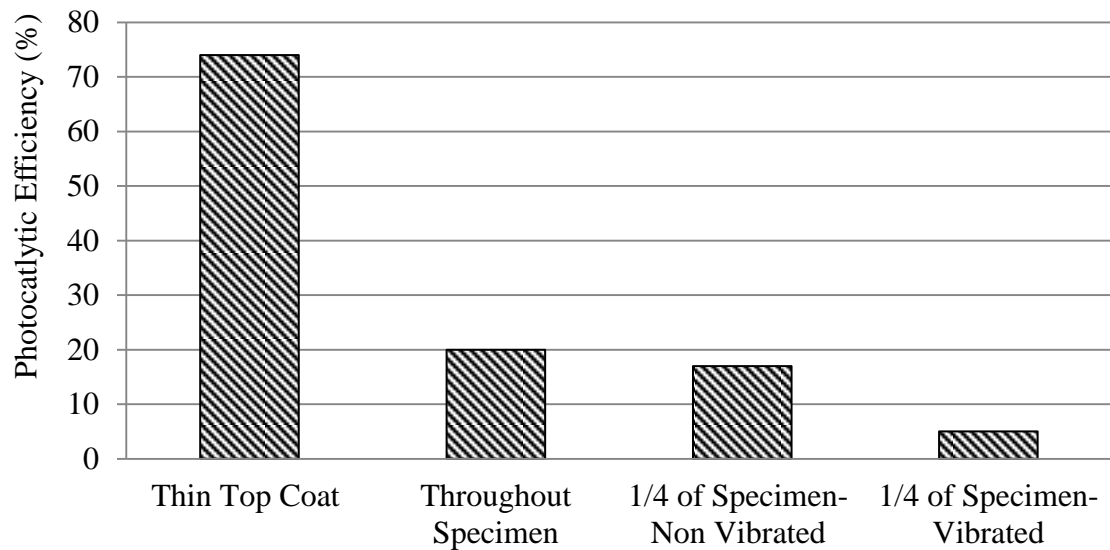


Figure 4.1 Effect of layer thickness containing TiO_2 on photocatalytic efficiency

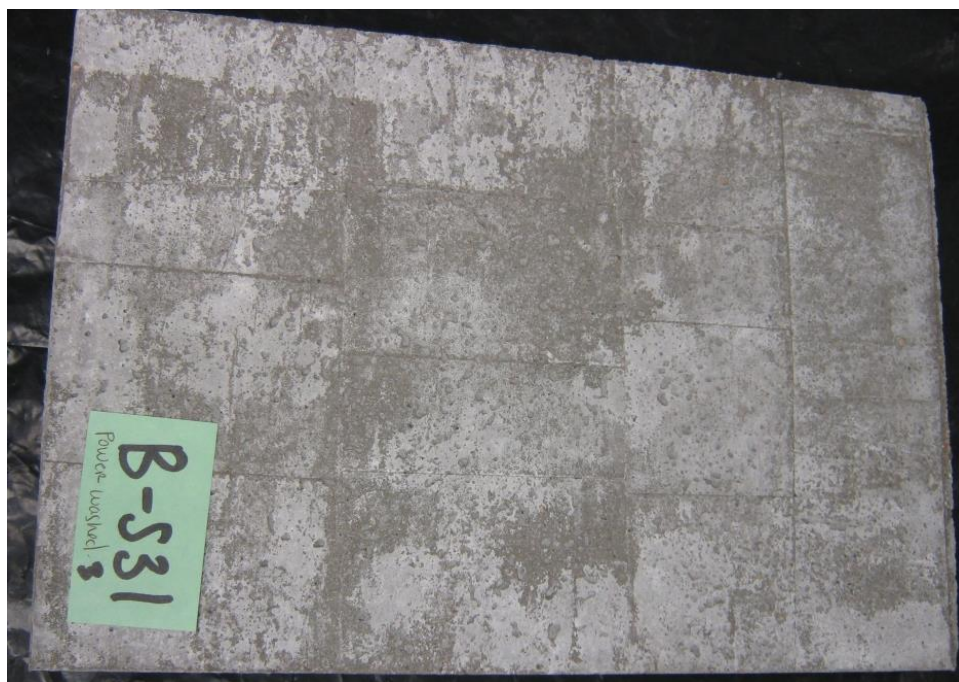


Figure 4.2 TiO_2 powder on gray cement specimen

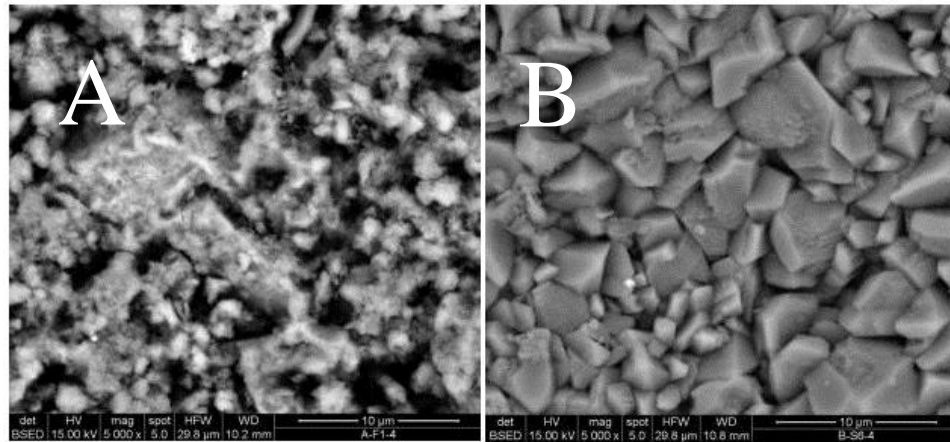


Figure 4.3 SEM of sample surfaces (A) Poorly cured (B) Properly cured specimen surface

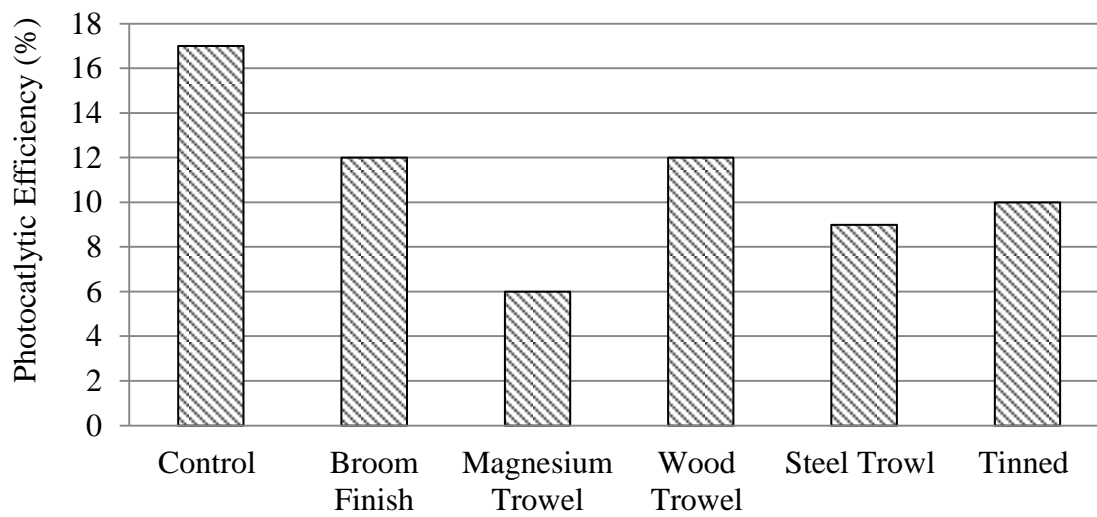


Figure 4.4 Fresh concrete finishing methods effects on photocatalytic efficiency

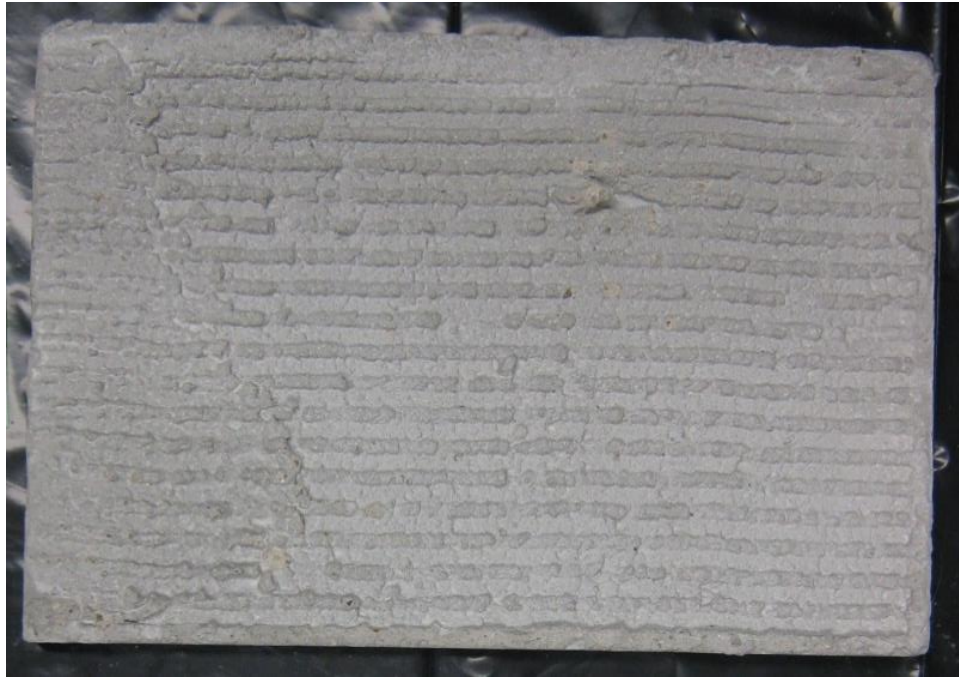


Figure 4.5 Tinned mortar surface specimen

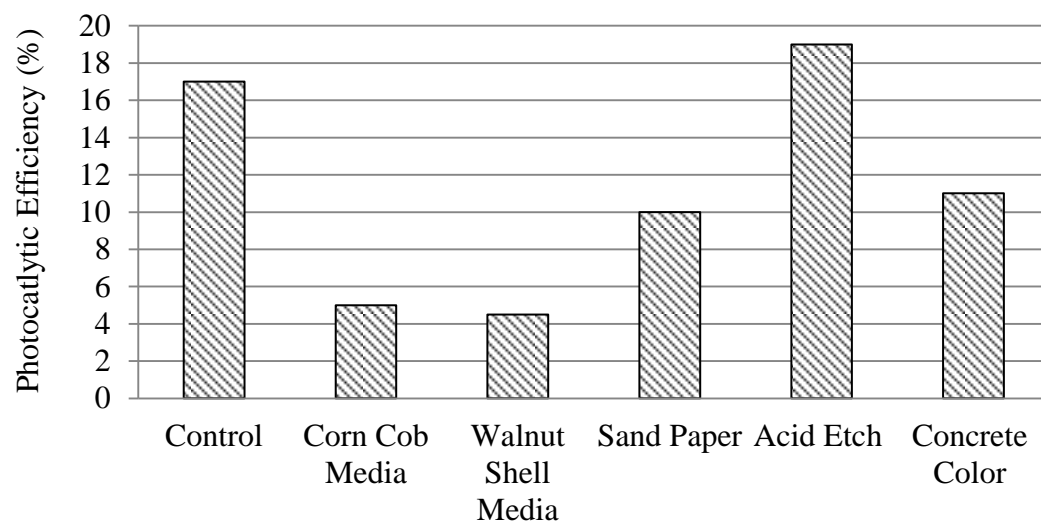


Figure 4.6 Effect of hardened mortar finishes on photocatalytic efficiency

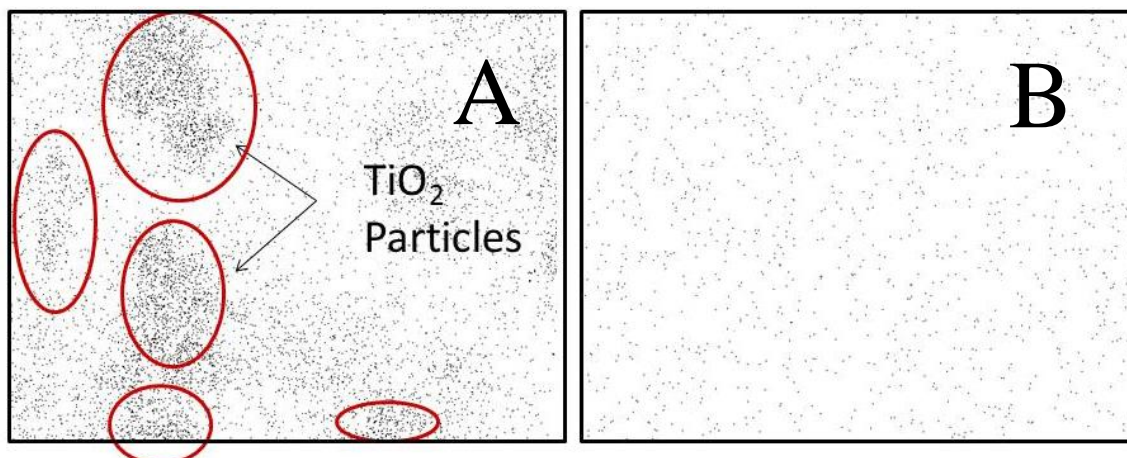


Figure 4.7 EDS of TiO₂ on surface of specimens (A) Control (B) Corn cob media blast

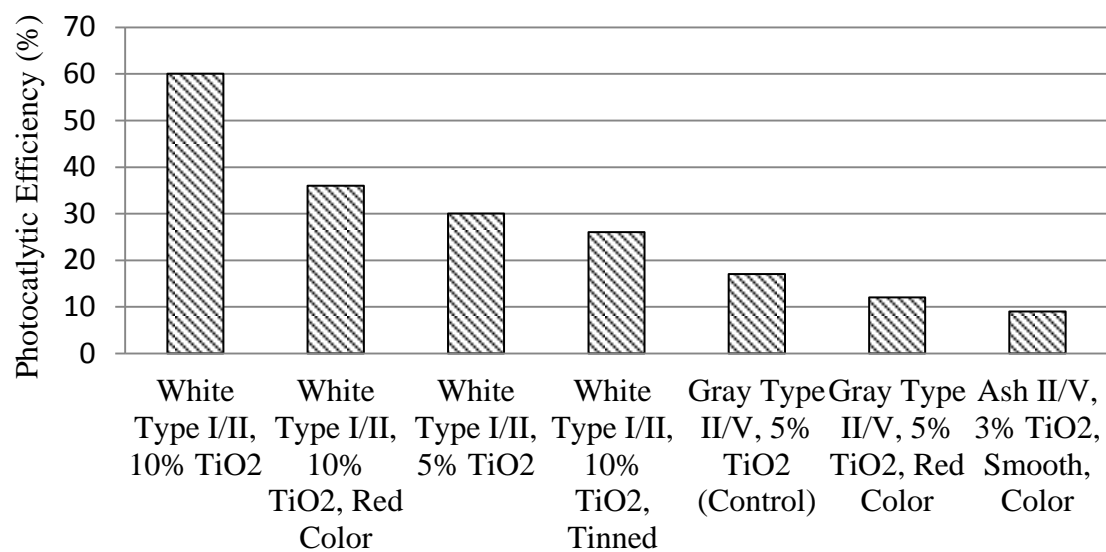


Figure 4.8 Effect of combining variable on photocatalytic efficiency

CHAPTER 5

REJUVENATION TECHNIQUES FOR CONCRETE CONTAINING PHOTOCATALYTIC TiO₂ MATERIAL

5.1 Abstract

Concrete has been shown to be a possible substrate in which photocatalytic titanium dioxide (TiO₂) can be mixed into the concrete matrix and after curing, can oxidize NO_x pollution gases. Concrete specimens containing TiO₂ were placed in two locations in Salt Lake City, UT, USA during two different seasons, winter and summer, for 120-days to be weathered. After being weathered, the specimens had an average photocatalytic efficiency reduction of 82% as compared to the photocatalytic efficiency before being weathered. Six rejuvenation methods were tested with the most effective method being muriatic acid washing, which returned the specimen to 60% of its initial photocatalytic efficiency. Phenolphthalein testing showed an accelerated carbonation rate for the surface that contained TiO₂. The carbonation material reduced the porosity and potentially covered the TiO₂ particles, contributing to the decreased efficiency with time.

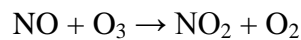
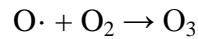
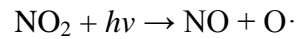
An unweathered control specimen was tested to verify the kinetics of specimens containing TiO_2 in the laboratory reactor system. The reactor system acted as a laminar flat plate flow with the rate of diffusion, rate of chemical reaction, and the residence time in the photo-reactor system playing roles in three visible trends. The three trends include the lower the flow rate is, the higher is the apparent photocatalytic efficiency. The lower the NO_x concentration is, the higher is the apparent photocatalytic efficiency. Finally, the rate of diffusion was rapid enough across the thin flow space in the photo-reactor that the difference in apparent photocatalytic efficiency between different NO_x concentrations was not affected by flow rate.

5.2 Background

5.2.1 Tropospheric Chemistry

The troposphere is the layer of the Earth's atmosphere nearest the Earth's surface and ranges from 7 to 8 km (4.3 to 5.0 mi.) at the poles to 16 to 18 km (10 to 11 mi.) near the Equator. Ozone smog in the troposphere is created through chemical reactions with nitrogen oxides (NO_x) and volatile organic compounds (VOC) that are emitted from automobile exhausts and emission from factories and power plants (Akbari and Berdahl, 2008). The NO_x gases in the troposphere are the primary source for oxygen radicals ($\text{O}\cdot$), which leads to the only significant source for ozone formation in the troposphere (Seinfeld and Pandis, 2006). Below are the chemical equations governing ozone formation. In the first equation, nitrogen dioxide (NO_2) reacts with photons of light ($h\nu$), forming nitric oxide (NO) and oxygen radicals ($\text{O}\cdot$). In the second equation, oxygen

radicals react with atmospheric oxygen (O_2), forming ozone (O_3). During the final equation, the nitric oxide reacts with ozone, forming nitrogen dioxide and oxygen.



If the three reactions occur at equal rates, a steady state ozone concentration is reached, which is called *photostationary state relations*. This steady state concentration is proportional to the NO_2 to NO ratio. The rate coefficient for the first equation depends on light intensity; therefore, it generally dominates during the daytime, which leads to the generation of O_3 . During the nighttime, there are no light photons to force the first equation, allowing the third equation to dominate. The rapid reaction between NO and O_3 results in NO_x gases being almost completely converted into NO_2 each night. These reactions play a major role in governing the diurnal rise and fall of ozone levels in the troposphere (Nazari and Riahi, 2011).

The U.S. Environmental Protection Agency's (EPA) National Ambient Air Quality Standard for nitrogen dioxide was changed in 2010, adding a new 1-hour 100 ppb standard in addition to the previously established 53 ppb annual requirement (U.S., 2012). Ozone near the earth's surface generally ranges from 20 to 60 ppb, with values exceeding 100 ppb in urban areas (Seinfeld and Pandis, 2006).

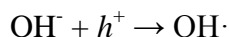
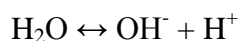
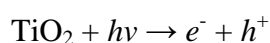
5.2.2 Photocatalytic Titanium Dioxide

Over the past decade, photocatalytic titanium dioxide (TiO_2) has been proven to be able to absorb and oxidize certain harmful pollutants such as NO_x in the presence of ultraviolet (UV) light through the formation of hydroxyl radicals ($\text{OH}\cdot$). It is speculated that each square meter of high-performance photocatalytic material exposed to outdoor sunlight can remove NO_x from 200 cubic meters of air per day (Akbari and Berdahl, 2008). TiO_2 can be manufactured into three different crystalline forms: rutile, anatase, and brookite. Anatase and rutile both have tetragonal di-tetragonal di-pyramidal crystal systems, which allows them to be n-type semiconductor photocatalyst, but only anatase has high photocatalytic properties under UV lights at intensities common on the earth's surface (Blimes et al., 2008; Hassan et al., 2010; Singh et al., 2012). Anatase photocatalytic abilities are contributed to the electron band energy gap (E_g) being 3.0 electron volts (eV) compared to rutile's 3.2 eV (Austin and Lim, 2008; Kavan et al., 1996).

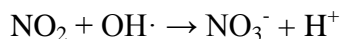
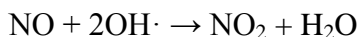
An n-type semiconductor has an electron filled valance band and an empty conduction band. When subjected to UV light, energy greater than E_g , an electron (e^-) from the valance band is excited to a higher energy state and moves from the valance band to the conduction band. When this move occurs, a positively charged vacant site in the valance band remains; this vacant site is called an electron-hole (h^+). The ability of the electrons in the conduction band to carry a moderate current makes the TiO_2 a semiconductor (Benedix et al., 2000; Dalton et al., 2002; Daude et al., 1977; Serway and Jewett, 2004). The electron-hole in the valance band then provides a site where adsorbed hydroxyl ions (OH^-) and disassociated water (H_2O) can lose an electron, which then

forms the hydroxyl radical ($\text{OH}\cdot$). Hydroxyl radicals are electrically neutral but highly reactive. The formation of the hydroxyl radical due to light photons through the movement of electrons is what classifies TiO_2 as a photocatalyst. The rate of formation and recombination between a positive hole and a free electron is considered to be very rapid (Hashimoto et al., 2000).

The symbolic chemistry for the formation of hydroxyl radicals follows:



Hydroxyl radicals are reactive with many of the trace species in the atmosphere while not being reactive with any of the major molecules of the atmosphere such as N_2 , O_2 , CO_2 , and H_2O (Seinfeld and Pandis, 2006). These trace species, including airborne pollutant molecules, can be adsorbed into the TiO_2 particle surface, where they react with the hydroxyl radicals and are oxidized (Berdahl and Akbari, 2008). One such trace species is nitric oxide (NO), which reacts with two hydroxyl radicals, forming one nitrogen dioxide (NO_2) and one water molecule. The nitrogen dioxide can then react with another hydroxyl radical, forming one nitrate (NO_3^-) and a one hydrogen ion. Figure 5.1 is a diagram of the entire process involving the TiO_2 and NO_x oxidation process. The symbolic chemistry of the NO_x oxidation process follows:



5.2.3 Field and Laboratory Studies

In Antwerp, Belgium, a test section of 10,000 m² (12,000 yd²) of pavement blocks was placed on the parking lanes of a main road. The blocks used contained TiO₂ in the weathering layer only. The concentration of nitrate deposited on the surface was measured and used to determine the minimum amount of NO and NO₂ that was oxidized. It was found that after 1-year, the air pollution reduction capabilities of the blocks had been reduced by 20% (Beeldens, 2006).

In Hengelo, Netherlands, a 750 m² (900 yd²) section of roadway was constructed using two lift precast blocks, where only the top 5 mm (0.2 in.) contained TiO₂. After construction was completed, the roadway did not show a significant decrease in the NO_x concentration when field samples were testing in the laboratory. To enhance the roadway surface, a coating containing suspended TiO₂ was sprayed onto the surface. After 2.5-months, the spray coating was gone due to outdoor exposure and vehicle wear. The surfaces' ability to reduce NO_x pollution had returned to prespray coating conditions. A second spray application was then used with similar results. With the base concrete containing TiO₂ and two spray application containing TiO₂, after 15-months of being exposed to weather and traffic, the concrete blocks were reducing the NO_x concentration in the laboratory by 3.6% compared to a peak performance of 60.2% after the second spray coating (Ballari and Brouwers, 2013).

The first US highway pavement project using TiO₂ was placed Missouri in 2011. The 460 m (1,500 ft) long, two lane road section was a two lift placement that contained a 5 cm (2 in) overlay of a commercially available white cement that contains TiO₂ (Cackler et al., 2011). After 1-year, surface capabilities to reduce NO_x pollutants were

lower than expected. To rejuvenate the surface, 1/8 inch diamond grinding was performed (Alleman, 2013).

Other studies being performed around the world are addressing other aspects of this developing technology that are important to help quantify potential environmental benefits from using concrete containing TiO_2 as well as other application methods of applying TiO_2 . One study to help quantify potential benefits includes a large-scale artificial canyon street lined with TiO_2 panels. Measurements taken from within the canyon containing TiO_2 were compared to a control canyon that did not contain TiO_2 . The canyon containing TiO_2 saw a reduction in NO_x concentrations of 36.7 to 82% (Maggos et al., 2008). Determining probable wide spread pollution reduction is difficult without computer modeling. Taking into account parameters such as 3D geometry, road traffic, effectiveness of pollution control, meteorology, and the pavement surfaces' efficiency to reduce NO_x pollutant concentrations, Overman (2009), from the Netherlands, created a computer model that shows that it is probable to have a NO_x pollution reduction of 30% at vehicle height and an overall NO_x pollution reduction of about 15% at a height of 20 m (65 ft) for a pavement containing TiO_2 (Overman, 2009). Another study using similar variables in a 2D model determined that at 1.5 m (5 ft) a NO_x reduction of 25% may occur (Rousseau et al., 2009).

Three alternative methods to mixing the TiO_2 into a typical concrete matrix include using paints (Barratt et al., 2012), spray coatings (Quagliarini et al., 2012), and pervious pavements (Hassan et al., 2012). Paint and spray coatings have high initial performance but are considered semipermanent and would have to be reapplied over the lifespan of the structure. Pervious pavements containing TiO_2 had an efficiency of 37 to

67% (Hassan et al., 2012). It was also concluded that the additional nitrate salts due to the oxidization of NO_x gases would not negatively impact the environment (Hassan et al., 2012).

Due to the variability of results of concrete containing TiO₂, research has begun to develop methods to increase concrete's natural ability to absorb NO_x pollutants through the addition of activated coal to the concrete mixture design. This method does not require ultraviolet light and therefore would be a more suitable solution for tunnel and parking garage applications where the NO_x concentrations and residence times are generally longer (Horgnies et al., 2012).

5.3 Experimental Program

The objective of this experimental program was to investigate the effect of weathering on specimens containing TiO₂. Due to the adverse effect of weathering, rejuvenation techniques to enhance the photocatalytic properties of concrete materials were addressed. Testing was also performed to verify the kinetics of the photocatalytic reaction by varying flow rates and NO_x concentrations in laboratory experiments.

5.3.1 Testing System and Procedure

The photo-reactor system developed to test laboratory specimens was designed based on a modified International Standard ISO 22197-1 "Fine ceramics (advanced ceramics, advanced technical ceramics) – Test method for air-purification performance of semiconducting photocatalytic materials," which was adapted from the Japanese Standard JIS TR Z 0018 "Photocatalytic materials – Air purification test procedures." These tests

standards call for using a chemiluminescent NO_x analyzer and an ion chromatograph for analysis of nitrate concentrations (ISO, 2007; JIS, 2002). The photo-reactor system contains an air tight stainless steel box with a glass top. The glass top enables UV light from four adjustable black lights to reach the specimens located inside the box. An air space of 5 mm (0.20 inch) exists between the bottom of the glass and the top of the specimen. NO_x contaminated air flows into the box, across the top of the specimen, and is exhausted. For all rejuvenation testing, the inlet NO_x concentration has held at 1.0 ± 0.1 ppm with a flow rate of 8 L/min. A chemiluminescent NO_x analyzer tests NO_x pollution concentrations from the exhaust line reservoir. During testing of the specimens, UV lights were adjusted so an average UV irradiance of $1300 \pm 50 \mu\text{W}/\text{cm}^2$ reached the surface of the specimens. $1300 \pm 50 \mu\text{W}/\text{cm}^2$ was chosen because it replicates the UV irradiance levels experienced by a sun exposed surface on a summer day. The relative humidity was held at 15% due to the results of previous studies, which showed that the photocatalytic reaction rate is more efficient at lower relative humidity (Dylla et al., 2010). The temperature was maintained at $25^\circ \pm 5^\circ \text{C}$ ($77^\circ \pm 10^\circ \text{F}$), typical laboratory temperatures. When testing the kinetic properties of the photocatalytic reaction, the temperature and UV irradiance levels were held constant at $25^\circ \pm 5^\circ \text{C}$ ($77^\circ \pm 10^\circ \text{F}$) and $1300 \pm 50 \mu\text{W}/\text{cm}^2$, respectively, while the flow rate was varied from 5 to 11 L/min and the NO_x pollution concentrations was varied from 0.3 ppm to 1.0 ppm. Figure 5.2 shows a schematic of the laboratory testing setup.

Testing was performed for 2-hours. The first and last 30-minutes, the UV lights were turned OFF to allow the system to stabilize and provide an initial NO_x concentration. At minute 30, the UV lights were turned ON and the system remained for

60 minutes. During this 60 minute period, an excited concentration was determined. A photocatalytic efficiency was determined for each test using the equation below:

$$\text{Photocatalytic Efficiency (\%)} = \frac{\text{Concentration}_{\text{initial}} - \text{Concentration}_{\text{excited}}}{\text{Concentration}_{\text{initial}}} \times 100$$

5.3.2 Materials and Methods

Concrete materials used for the production of test specimens included ASTM C150 Type II/V and White Type I/II portland cements along with ASTM C33 fine aggregate concrete sand, which had a fineness modulus and absorption of 2.90 and 1.9%, respectively. The mortar was mixed following the procedures of ASTM C109 with a constant water to cement ratio of 0.485. Test specimens were 0.929 m² (1 ft²) by 1.9 cm (0.75 in.) thick, trowel finished, and wet cured for 14-days.

The photocatalytic TiO₂ used for this project is 96.5% TiO₂ with a mean particle size of 1.0 µm. The TiO₂ is considered an aggregate and each specimen contained 5% TiO₂ by mass percentage of cement.

Three groups of specimens were weather tested. Two groups were placed in April and collected in August. The third group was placed in October and collected in February. In Salt Lake City, Utah, USA, the average high temperature and rainfall during the summer and winter testing periods was 29° C (84° F) with 0.81 in. of rainfall per month and 7° C (45° F) with 1.35 in. of rainfall per month, respectively (National, 2013). These time periods were chosen as they are the two seasons with the highest NO_x concentrations and with the most distinctive weather climates. The orientation of specimens was also considered. The two summer groups contained specimens that were weathered in both the vertical and horizontal position. One summer group was placed

approximately 10 m (33 ft) from a busy highway which runs adjacent to Interstate 15 in Salt Lake City. The second group of summer specimens and the winter group were placed on the roof of a campus building at the University of Utah, which is also located in Salt Lake City.

After the weathering period had been completed, the specimens were returned to the laboratory and tested for photocatalytic efficiency. Due to their significant decrease in photocatalytic efficiency, potential methods to return the specimens to initial “pre-weathered” photocatalytic efficiency were investigated. These methods included rinsing, power washing, oven drying, acid washing, walnut media blasting, and hand sanding. Rinsing was done with 200 mL (6.75 oz) of water per specimen. 200 mL was chosen because it sufficiently removed loose particles from the specimen surface. Power washing was done with $18,615 \text{ kN/m}^2$ (2,700 psi) of pressure for 10 seconds per 0.929 m^2 (1 ft^2) at a distance of 0.25 m (8 in.). Increases in pressure and duration or decreases in distance visually did not remove any additional surface particles. Oven-dried specimens were placed in a vented oven at 80° C (175° F) for 24-hours. After 24-hours, the specimens were allowed to cool for 1-hour at room temperature before being tested.

Media blasting was the next method tested. Walnut shells were chosen over more standard media blasting materials such as silica sand or slag due to the safety and environmental concerns. Silica sand is considered dangerous due to its tendency to break up quickly, which causes large amounts of suspended fine particles that if inhaled can cause silicosis, and serious lung disease. Slag is a safer material but as a rejuvenation technique, large-scale use in a noncontrolled environment is unacceptable because of the negative environmental effect of the slag dust, which is difficult to remove. As a safer

and natural alternative, fine walnut shell blown at 415 kN/m^2 (60 psi) from a distance or 0.20 m (8 in.) for 30 seconds was used. The material is relatively soft and the blast media debris is biodegradable so no cleanup would be required for large-scale use in non-controlled environments. The final method is hand sanding. Hand sanding was done with medium grit sand paper using moderate pressure. The surface was sanded so each unit of surface was sanded with 6 passes. Acid etching was done with muriatic acid, a typical acid used for concrete etching and cleaning, at a concentration of 8% following manufactures recommendations.

5.4 Experimental Results and Discussion

5.4.1 Weathered Specimens

After each 120-day weathering cycle, the specimens were returned to the laboratory to be tested and compared with their initial photocatalytic efficiency before being weathered. Average initial photocatalytic efficiency for the samples was 30%. The average efficiency of the summer weathered samples was 7%. There was no evidence that the specimens that were weathered horizontally had any significant difference in photocatalytic efficiency reduction as the specimens that were weathered vertically. Likewise, there was no significant difference between the samples that were weathered near the highway and interstate and those weathered on the roof of a building. The specimens that were weathered during the winter months saw an 86% efficiency reduction compared to the summer specimens, which averaged 77% reduction.

5.4.2 Rejuvenation Techniques

Due to the significant reduction in photocatalytic efficiency of the specimens, testing was performed to identify possible techniques to rejuvenate the concrete surface back to initial photocatalytic efficiencies. Figure 5.3 shows the results of the initial, after weathering, and six rejuvenation methods tested. Rinsing the specimens removed some of the particulates but did not increase the photocatalytic efficiency of the specimen. Rinsing was increased to power washing to remove more of the surface particles. Power washing did provide a slight increase in photocatalytic efficiency. This increase is attributed to the removal of a higher quantity of particulates that allows for more UV light to reach the surface, which is the driving force of the photocatalytic reaction and therefore increased the photocatalytic efficiency. The photocatalytic cycle is not as efficient in high humidity conditions as in low humidity conditions, so specimens were oven dried at 80° C (175° F) for 24-hours. Drying the specimens did have an effect of partially returning the photocatalytic efficiency for a short time. During the 2-hour testing period, there was a noticeable decrease in photocatalytic efficiency. The 17% photocatalytic efficiency reported in Figure 5.3 is the efficiency seen over the 2- hour timeline of the testing parameters. This quick decrease in photocatalytic efficiency eliminates the method of drying as a possible rejuvenation technique. However, it does lead to the understanding that water molecules are interacting with the photocatalytic cycle and kinetics of the system.

The next three rejuvenation methods altered the surface of the specimens. The first two methods were media blasting with walnut shells and sanding. These techniques did have a small effect by increasing the photocatalytic efficiency to 10 and 9%,

respectively, but this increase only brought the surface to approximately 33% of the initial photocatalytic efficiency. Both methods remove a thin layer of the concrete surface, which has the potential to expose new particles of TiO_2 , but it also has the potential to remove the TiO_2 particles from the surface. The minimal rejuvenation of these methods is contributed to the layer of concrete paste removed being too thin to provide any substantial change in photocatalytic efficiency; however, if more aggressive methods were utilized that remove a thicker layer of concrete paste, the potential for the removal of TiO_2 particles on the surface may increase.

The final rejuvenation method was acid washing with muriatic acid. Muriatic acid etching returned the specimen photocatalytic efficiency to 18%, which is 60% of the initial efficiency. The reason for the increase is due to the removal of a layer of cement on the surface. Muriatic acid is neutralized by the calcium in the cement and dissolves a layer of cement. The removal of a cement layer reveals a new layer of TiO_2 that can begin reacting with NO_x gases again. This technique was the most effective rejuvenation method tested. However, it is an unlikely solution to the weathering effect of surfaces containing photocatalytic TiO_2 as it has a pH of less than 1.0, will burn eyes and skin if it comes into contact, and will react with caustic materials, oxidizing materials, and metals such as galvanized iron, brass, aluminum, copper, and copper alloys.

Upon further investigation into the mechanisms that are causing the weathered specimens to have a reduction in photocatalytic efficiency, weathered specimens were cut in half and tested for carbonation using phenolphthalein. Figure 5.4 shows a typical cross-section of a vertically weathered test specimen that has been sprayed with

phenolphthalein. Phenolphthalein is an indicator of the pH of the concrete surface. The higher the pH is, the darker the phenolphthalein becomes. The thickness of the light layer is the depth to which the concrete has carbonated. Concrete carbonation is caused by the carbon dioxide (CO_2) in the air reacting with the calcium hydroxide ($\text{Ca}(\text{OH})_2$) in the cement paste, which forms calcium carbonate (CaCO_3). Carbonation reduces the pH of the concrete to around 7, which reduces its ability to resist corrosion. It is assumed that good quality concrete will have on average 1 mm (0.04 in.) of carbonation during its first year (Vaysburd et al., 1993). The top 5 mm (0.2 in.) layer of this test specimen contains 5% TiO_2 by cement mass and the rest of the specimen does not contain TiO_2 . The bottom surface that does not contain TiO_2 had approximately 1.3 mm (0.05 in.) of carbonation after the 120-day weathering period. This depth of carbonation is slightly higher than the predicted depth of carbonation for good quality concrete due to the relatively high water-to-cement ratio of 0.485 used in the mortar mixture. The top layer that contained TiO_2 had a carbonation penetration of approximately 2.5 mm (0.10 in.). The accelerated carbonation of the surface layer containing TiO_2 is assumed to be caused by the increased concentration of CO_2 on the concrete surface. Carbon monoxide (CO) is a major trace element in the troposphere that also reacts with the hydroxyl radical formed by the TiO_2 particles, leading to the formation of CO_2 , the main driver of concrete carbonation (Seinfeld and Pandis, 2006).

The rapid carbonation of the concrete that contains TiO_2 is one of the major contributors to the specimen's reduction in photocatalytic efficiency. The carbonation decreases the porosity of the concrete that reduces the overall surface area, leading to fewer TiO_2 particles having sufficient UV irradiation and air flow across the particle

surface to oxidize the NO_x gases. The calcium carbonate on the surface also appears to be covering the TiO₂ particles. To help quantify the changes in surface chemical characterization, energy-dispersive X-ray spectroscopy (EDS) was utilized. EDS only measures the elemental surface concentration to a depth of 2 μm. There was a 60% relative reduction in surface titanium and a 10% relative increase in calcium in the 2 μm surface layer. The increase in calcium is expected to be due to the carbonation process. The calcium carbonate created during carbonation is covering the titanium particles, which cause the surface concentration of the calcium to increase and the surface concentration of the titanium to decrease.

5.4.3 Kinetics of NO_x Reaction

Using a single specimen, the kinetics of the system was investigated. The laboratory setup creates a 1-directional laminar flow system. Three factors affect the kinetics of the system. First is the area and volume of the photo-reactor system, which affects the residence time. Second is the rate of diffusion to the surface, which is driven by the difference in NO_x pollution concentration at the surface of the concrete specimen and the concentration of the general mass of air passing over the specimen. As the difference in concentrations increases, the rate of diffusion increases. Third is the rate of chemical reaction, which influences the reaction time of a NO_x particle and the hydroxyl radical. Although all three factors influence the kinetics of the system continually, trends can be influenced by a particular factor.

Figure 5.5 shows the apparent photocatalytic efficiency of the specimen due to changes in flow rate and NO_x pollutant concentration. Three trends are visible from this

data. The first trend is the slower the flow rate, the higher the apparent photocatalytic efficiency of the surface. This trend is influenced by the changes of the residence time of the molecules in the photo-reactor system. When the flow rate is higher, the potential time frame for chemical reactions to occur at a particular point of the air flow is decreased leading to lower apparent efficiencies.

The second trend is lower concentrations of NO_x pollutants have higher apparent photocatalytic efficiency than higher NO_x concentration experiments. This trend is partially governed by the rate of reaction in the system. The rate of reaction, units of moles liter⁻¹ second⁻¹, defines the change in concentration of the reactants or products per unit of time. When the photo-reactor system is limiting the quantity of NO_x molecules being oxidized, experiments with lower concentrations of NO_x molecules have a higher percentage of the NO_x molecules oxidized, leading to higher apparent photocatalytic efficiency.

The final trend is the difference in concentration between apparent photocatalytic efficiency for each flow rate at 0.3 and 1.0 ppm is approximately 10%. This consistent difference in apparent efficiency shows that the rate of diffusivity remains stable at different flow rates for a particular NO_x concentration. The narrow space between the top of the specimen and the bottom of the glass is small enough that the air flow through the system has a relatively uniform NO_x concentration gradient.

5.5 Conclusions

- 1) The photocatalytic efficiency of concrete specimens that contain photocatalytic TiO₂ significantly decreased when exposed to the environment

of an urban city for 120-days. The season and orientation of the testing regiment did not significantly change the effect of being exposed to weather.

- 2) Rejuvenation techniques including power washing, media blasting, acid washing and sanding were investigated. Acid washing the surface was the most effective rejuvenation technique. However, it only returned the specimen surface to 60% of its initial photocatalytic efficiency.
- 3) The decrease in photocatalytic efficiency of the weathered specimens is partially attributed to carbonation of the concrete surface. The concrete carbonation reaction generates calcium carbonate, which increased the density of the concrete matrix as well as covers the TiO_2 particles, leading to less TiO_2 particles available for the NO_x oxidation cycle.
- 4) The rate of chemical reaction, rate of diffusion, and the area of the sample all play a role in the kinetics leading to the apparent photocatalytic efficiency of a specimen. Apparent photocatalytic efficiency increases when the NO_x pollutant concentration decreased and when the flow rate decreases. The difference in apparent efficiency between 0.3 ppm and 1.0 ppm stays relatively consistent for all three flow rates tested.

5.6 References

- Akbari, H.; Berdahl, P. *Evaluation of Titanium Dioxide as a Photocatalyst for Removing Air Pollutants*. Technical Report for the Public Interest Energy Research Program California Energy Commission: Berkeley, CA, January 2008.
- Alleman, J. The Science and Engineering of Photocatalytic Pavements: Update on 1st US 'TX Active' Highway Application. Proceedings of the International Concrete Sustainability Congerence, San Francisco, May 2013.

- Austin, R.; Lim, S. The Sackler Colloquium on Pormoses and Perils in Nanotechnology for Medicine. *Proceedings of the National Academy of Science* **2008**, *105*, 17217-17221.
- Ballari, M.; Brouwers, H. Full Scale Demonstration of Air-Purifying Pavement. *Journal of Hazardous Materials* **2013**, *254*, 406-414.
- Barratt, B.; Carslaw, D.; Green, D. *High Holborn D-NOx Paint Trial- Report 3 (Updated)*; Technical Report for King's Colledge London Environmental Research Group: London, 2012.
- Beeldens, A. *An Environmental Friendly Solution for Air Purification and Self-Cleaning Effect: the Application of TiO₂ as Photocatalyst in Concrete*; Technical Report for Belgian Road Research Centre: Brussels, Belgium, 2006.
- Benedix, R.; Dehn, F.; Quaas, J.; Orgass, M. Application of Titanium Dioxide Photocatalysis to Create Self-Cleaning Building Materials. *Lacer* **2000**, *5*, 157-168.
- Berdahl, P.; Akbari, H. *Evaluation of Titanium Dioxide as a Photocatalyst for Removing Air Pollutants*. Technical Report for PIER Energy-Related Environmental Research Program California Energy Commission: Berkeley, CA, 2008.
- Blimes, S.; Mandelbaum, P.; Alvarez, F.; Victoria, N. Surface and Electronic Structures of Titanium Dioxide Photocatalyst. *Journal of Physical Chemistry B* **2008**, *104*, 9851-9858.
- Cackler, T.; Alleman, J.; Kevern, J.; Sikkema, J. *Environmental Impact Benefits with "TX Active" Concrete Pavement in Missouri DOT Two-Lift Highway Construction Demonsration*; DTFH61-06-H-00011; National Concrete Pavement Technology Center; Ames, IA, 2011.
- Dalton, J.; Janes, P.; Jones, N.; Nicholson, J.; Hallam, K.; Allen, G. Photocatalytic Oxidation of NO_x Gases Using TiO₂: a Surface Spectroscopic Approach. *Environmental Pollution* **2002**, *120*, 415-422.
- Daude, N.; Gout, C.; Jouanin, C. Electronic Band Structure of Titanium Dioxide. *Physical Review B* **1977**, *15*(6), 3229-3235.
- Dylla, H.; Hassan, M.; Mohammad, L.; Rupnow, T.; Wright, E. Evaluation of Environmental Effectiveness of Titanium Dioxide Photocatalyst Coating for Concrete Pavement. *Transportation Reserach Record* **2010**, 46-51.

- Hashimoto, K.; Wasada, K.; Toukai, N.; Kominami, H.; Kera, Y. Photocatalytic Oxidation of Nitrogen Monoxide Over Titanium Oxide Nanocrystals Large Size Areas. *Journal of Photochemistry and Photobiology A: Chemistry* **2000**, *136*, 103-109.
- Hassan, M.; Dylla, H.; Mohammad, L.; Rupnow, T. *Effect of Application Methods on the Effectiveness of Titanium Dioxide as a Photocatalyst Compound to Concrete Pavement*. Proceedings of the Transportation Research Board, Washington, D.C., 2010.
- Hassan, M.; Asadi, S.; Kevern, J.; Rupnow, T. Nitrogen Oxide Reduction and Nitrate Measurements on TiO₂ Photocatalytic Pervious Concrete Pavement. *Construction Research Congress*. West Lafayette, LA, 2012.
- Horgnies, M.; Dubois-Brugger, I.; Gartner, E. NO_x De-Pollution by Hardened Concrete and the Influence of Activated Charcoal Additions. *Cement and Concrete Research* **2012**, *42*, 1348-1355.
- ISO 22197-1, International Standard ISO. "Fine Ceramics (Advanced Ceramics, Advanced Technical Ceramics) - Test Method for Air-Purification Performance of Semiconducting Photocatalytic Materials Part 1: Removal of Nitric Oxide." 2007.
- Jayapalan, A.; Lee, B.; Fredrich, S.; Kurtis, K. Influence of Additions of Anatase TiO₂ Nanoparticles on Early-Age Properties of Cement Based Materials. *Journal of the Transportation Research Board* **2010**, 41-46.
- JIS 0018:2002, Japanese Industrial Standards TR Z. "Photocatalytic Materials -- Air Purification Test Procedure ." 2002.
- Kavan, L.; Gratzel, M.; Gilbert, S.; Klemen, C.; Scheel, H. Electrochemical and Photoelectrochemical Investigation of Single-Crystal Anatase. *Journal of the American Chemical Society* **1996**, *118*, 6716-6723.
- Maggos, T.; Plassais, A.; Bartzis, J.; Vasilakos, N.; Moussiopoulos, N.; Bonafous, L. Photocatalytic Degradation of NO_x in a Pilot Street Canyon Configuration using TiO₂- Mortar Panels. *Environmental Monitoring and Assessment* **2008**, *136*, 35-44.
- National Weather Service Forecast Office: Observed Weather Reports: National Oceanic and Atmospheric Administration.
<http://www.nws.noaa.gov/climate/index.php?wfo=slc> (accessed July 29, 2013).
- Nazari, A.; Riahi, S. The Effects of TiO₂ Nanoparticles on Properties of Binary Blended Concrete. *Journal of Composite Materials* **2011**, *45(11)*, 1181-1188.

- Overman, H. Simulation Model for NO_x Distributions in a Street Canyon with Air Purifying Pavement. Thesis, University of Twente, Enschede, the Netherlands, 2009.
- Quagliarini, E.; Bondioli, F.; Goffredo, G.; Cordoni, C.; Munafo, P. Self-Cleaning and De-Polluting Stone Surfaces: TiO₂ Nanoparticles for Limestone. *Construction and Building Materials* **2012**, *37*, 51-57.
- Rousseau, P.; Drouadaine, I.; Maze, M. Le Procédé NO_xer: du Développement Aux Mesures de Depollution sur Site. RGRA-Revue Generale des Routes et des Aerodromes **2009**, *876*, 80-85.
- Seinfeld, J.; Pandis, S. *Atmospheric Chemistry and Physics From Air Pollution to Climate Change*; John Wiley & Sons, Inc.: New Jersey, 2006.
- Serway, R.; Jewett, J. Electrical Conduction in Metals, Insulators, and Semiconductors. In *Physics for Scientists and Engineers with Modern Physics*; Brooks/Cole-Thomson Learning: Belmont, 2004; pp 1420-1424.
- Singh, A.; Hanisch, J.; Matias, V.; Ronning, F.; Mara, N.; Pohl, D.; Rellinghaus, B.; Reagor, D. Transforming Insulating Rutile Single Crystal into a Fully Ordered Nanometer-Thin Transparent Semiconductor. *Nanotechnology* **2010**, *21*, 1-5.
- U.S. Environmental Protection Agency: National Ambient Air Quality Standards (NAAQS). <http://www.epa.gov/air/criteria.html> (accessed March 26, 2012).
- Vaysburd, A.; Sabnis, G.; Emmons, P. Concrete Carbonation - A Fresh Look. *Indian Concrete Journal* **1993**, *67(5)*, 215-220.

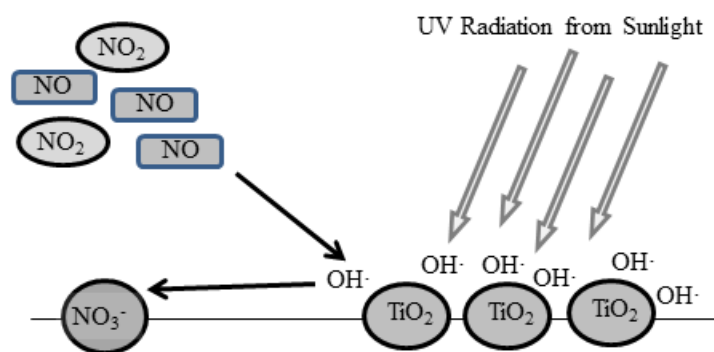


Figure 5.1 Photocatalytic titanium dioxide oxidation of NO_x gas pollutants

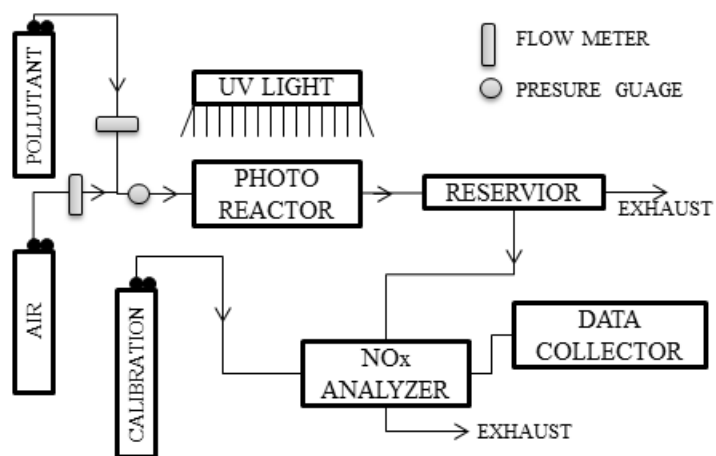


Figure 5.2 Laboratory testing setup schematic

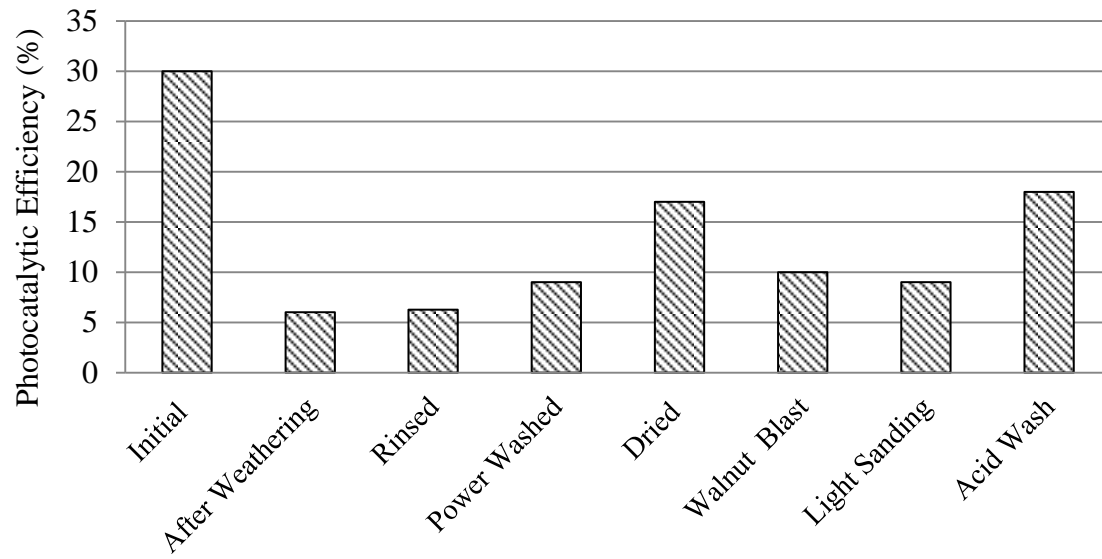


Figure 5.3 Results from surface rejuvenation techniques

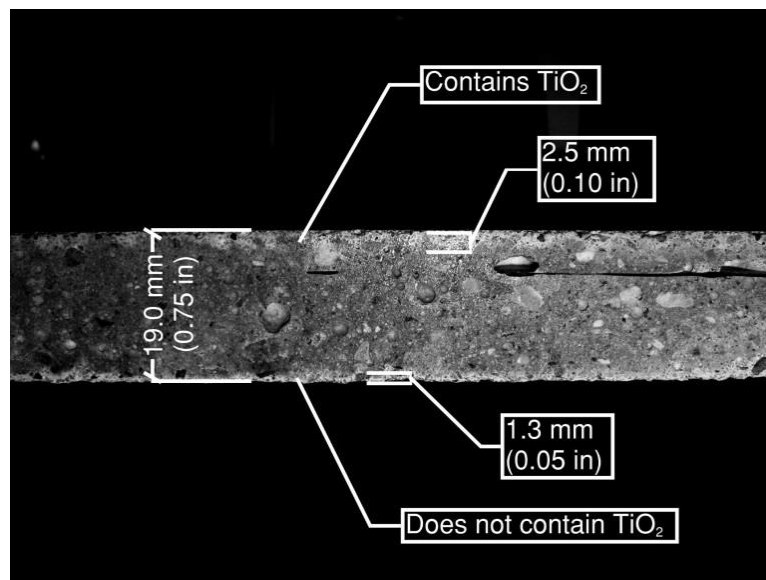


Figure 5.4 Test for surface carbonation for specimen that contains TiO_2 photocatalytic materials using phenolphthalein.

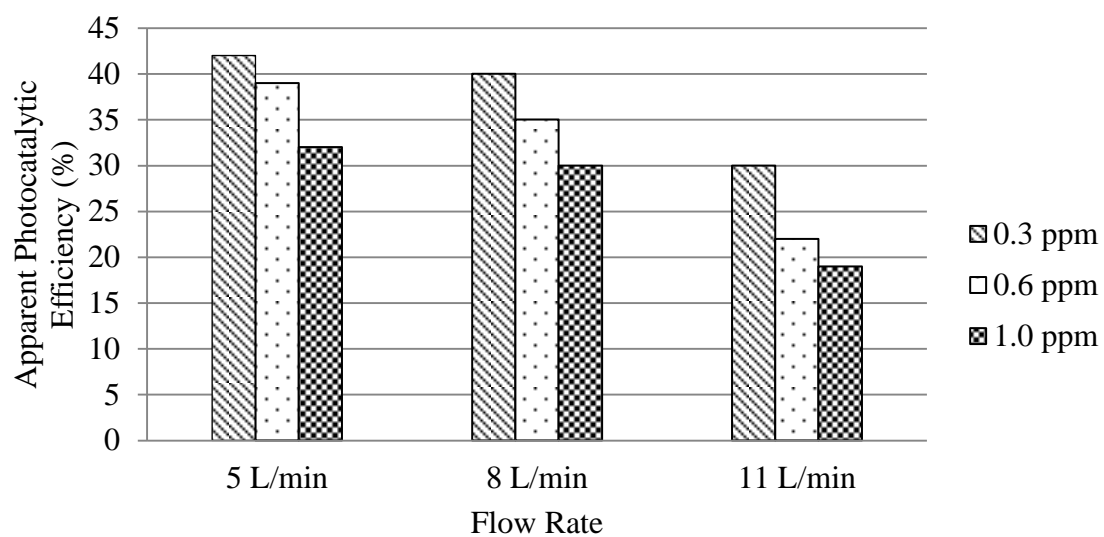


Figure 5.5 Apparent photocatalytic efficiency due to changes in flow rate and NO_x concentration

CHAPTER 6

PRECAST CONCRETE APPLICATIONS

6.1 Abstract

An architectural precast producer added TiO_2 to three of their current manufacturing techniques. The addition of TiO_2 affected the texture of the concrete and required additional superplasticizer to achieve the same workability. The most effective and cost-efficient method was adding the TiO_2 to a color slurry that was painted into the mold before being backfilled with typical grey concrete. Media blasting and concrete color reduces the photocatalytic efficiency of the specimen.

6.2 Introduction

Unlimited Designs, Inc., an architectural precast producer located in Salt Lake City, Utah, joined efforts with the University of Utah to test the manufacturing applicability of using TiO_2 in their current manufacturing processes. Laboratory testing samples were made using three different manufacturing techniques. The influence of color and typical finishing techniques were also investigated. The TiO_2 used for the specimens created with Unlimited Designs was Cristal Global PC 105, a TiO_2 with 95wt.% TiO_2 with a surface area of $90 \text{ m}^2/\text{g}$. The price of this product was quoted on July 6, 2012 to be \$3,000/100 kg for their *Large Sample* size.

6.3 Experimental Program

Three manufacturing techniques were investigated: thin façade paneling, glass fiber reinforced concrete (GFRC) façade paneling, and faux brick veneer. The thin façade paneling utilized a relatively typical concrete mixture design of 1 part cement to 2 parts fine aggregate to 2.9 parts coarse aggregate to 0.38 parts water. 5% TiO_2 by cement mass was added to the entire mixture. The paneling was then vibrated for compaction, as seen in Figure 6.1. The panels were cast so the finished surface was on the bottom of the form. This allows Unlimited Designs to produce a wide range of finished textures from extremely smooth, to wood textured, to elaborately decorative. This method is used for creating faux siding, pavers, and other decorative finishes. The testing samples made from this procedure were made of both Holcim Type I/II and TXI Type III cement. Color was added to the Type III cement mixture design. The surface chosen for testing was *smooth* as it is one of their typical manufacturing surfaces. Due to the duration of vibration, approximately 3 minutes, and the typical procedure of only using a one lift system, the panels required a high quantity of TiO_2 . It was estimated that each 1 ft^2 specimen contained 30 g of TiO_2 , which would increase the cost of the 1 ft^2 specimen by \$0.90.

The second manufacturing technique was a two lift spray up operation utilizing GFRC. Due to the size of the specimens, this technique was mimicked without using the glass fiber sprayers. The first coat is approximately $\frac{1}{4}$ inch thick and contains high quantities of white cement with, silica sand, water, and Latex, with a water-to-cement ratio of 0.36. Any concrete coloring or special aggregates that are to be revealed by media blasting are also added to this initial layer. After the first layer is roughly placed in

the mold, it is smoothed with a paint brushed to remove any air voids and create a consistent thickness, as seen in Figure 6.2. This initial layer is the layer exposed to the environment and is the layer which contains 5% TiO_2 by cement mass. The second layer is approximately $\frac{1}{2}$ inch and contained higher quantities of GFRC for strength and durability. Figure 6.3 shows the second layer being added to the form where it will be completely filled. 24-hours after being cast, some of the GFRC panels were media blasted with silica sand to add texture and reveal the aggregate. Due to the high cement content of the initial layer, this method had a cost increase of \$0.80 per square foot.

The final method creates faux brick veneers. To color the bricks, a fluid, high paste content mortar slurry containing the color is painted into the forms, as seen in Figure 6.4, then back filled with concrete. TiO_2 was added to this slurry layer at 10% TiO_2 by cement mass of the slurry mixture, which would increase the cost of this product by approximately \$0.025 per square foot. This method uses the least amount of TiO_2 and is produced in the largest quantities so it would have the highest potential environmental impact for the least amount of cost. The brick veneers are mass produced unlike the previous two methods, which are special order only. Figure 6.5 shows what the brick veneer specimens look like after being removed from their molds.

After being cast, typical curing procedures were followed for each manufacturing method, and de-molding occurred at approximately 24-hours. Media blasting, if utilized, occurred rapidly after demolding while the concrete was still relatively green. Muriatic acid etching at 10% concentration is also a common technique.

All of the test specimens produced were made into 1ft^2 specimens that fit into the photo-reactor system. The specimens were tested at a minimum of 7-days after being

cast. The specimens were tested with an air flow rate of 8 L/min, NO_x pollution concentration of 1.0 ppm, temperature of 25°C, relative humidity of 15%, and UV irradiance of 1300 $\mu\text{W}/\text{cm}^2$. The specimens were tested for 2-hours each. The first and last 30 minutes, the UV lights were turned OFF, while during the middle hour, the lights were turned ON. A photocatalytic efficiency was determined for each test.

6.4 Experimental Results and Discussion

6.4.1 Construction Techniques

Three construction techniques were investigated. When TiO₂ was added at 5% to the thin paneling, there was a noticeable increase in the stickiness of the mortar, which is due to the small particle size of the TiO₂. The change in texture was similar to what occurs when adding silica fume to a concrete mixture. To maintain workability, additional super plasticizer was added before the specimens could be cast. The workability of the GFRC and brick veneer manufacturing techniques did not appear to be as affected by the addition of the TiO₂.

The addition of the white TiO₂ did affect the tint of the gray concrete. Color variation is a common concern when constructing architectural panels as each panel may need to be identical in color. To keep the color consistent, white cement is often used because it does not have the color variation which occurs with gray cements. The white cement color is not affected by the addition of white TiO₂. If the project requires a gray cement base color, potential color variation due to the addition of TiO₂ would need to be addressed.

Figure 6.6 shows the photocatalytic efficiency of the samples for the different manufacturing methods.

The specimen with the highest photocatalytic efficiency was the thin panel specimens with a smooth finish, which had a photocatalytic efficiency of 35%. The GFRC specimens had a photocatalytic efficiency of less than half of the thin panel. This decrease is likely due to the changes in mixture design. The GFRC specimens have a 1:1 ratio of cement to fine aggregate. The higher cement content led to a large percentage of the TiO_2 particles being covered by the cement paste product reducing its photocatalytic efficiency.

The brick veneer specimens had moderate photocatalytic efficiencies with an average of 22%. This manufacturing process used the least amount of TiO_2 per square foot and had reasonable results. Adding TiO_2 to these specimens also did not require the water-to-cement ratio to be adjusted nor require additional admixtures to maintain workability.

6.4.2 Finishing Techniques

Many of the products sold by Unlimited Designs incorporate some type of finishing. The three main techniques that were investigated were acid etching, coloring, and media blasting. Acid washing and adding color to the panel reduced the photocatalytic efficiency of the thin panel construction method. These reductions were expected due to previous testing.

The final method was media blasting with silica sand. Previous laboratory testing using walnut shells or corn cob had negatively impacted the photocatalytic efficiency of

the specimens; however, the use of silica sand slightly increased the photocatalytic efficiency of the GFRC specimens. The remaining finish of the GFRC specimen was much different than the finish after using silica sand. Figure 6.7 shows a GFRC specimen before with no surface treatment on the left and a specimen after being media blasted with silica sand on the right. The right specimen shows how an entire layer of cement paste has been removed exposing the fine aggregate of the GFRC. The surface area of the GFRC specimen now exposed to the atmosphere contains both cement paste and fine aggregate, which reduces the area available for TiO_2 to be exposed due to it being mixed into the cement paste. However, the silica sand blasting has potentially revealed a higher density quantity of TiO_2 particles in the cement paste so that the photocatalytic efficiency did not decrease when the surface area of cement paste decreased.

6.5 Conclusion

Adding photocatalytic TiO_2 to current architectural precast manufacturing techniques is possible and can be economical. The fineness of the TiO_2 particles does reduce the workability of the concrete mixture stickier, which may require changes to the mixture design to maintain workability. Manufacturing techniques that utilize a lift system decrease the additional cost associated with adding TiO_2 to the mixture design as only a portion of the product would contain TiO_2 instead of having TiO_2 throughout the product thickness. Acid etching and adding concrete color decreases the photocatalytic efficiency while media blasting with silica sand may not negatively affect the photocatalytic efficiency of the product.



Figure 6.1 Thin façade paneling specimens being vibrated for compaction



Figure 6.2 Initial layer of GFRC specimen being smoothed with a paintbrush



Figure 6.3 Second layer of GFRC specimen being placed into mold



Figure 6.4 Brick veneer specimens with slurry layer applied



Figure 6.5 Brick veneer specimens after curing

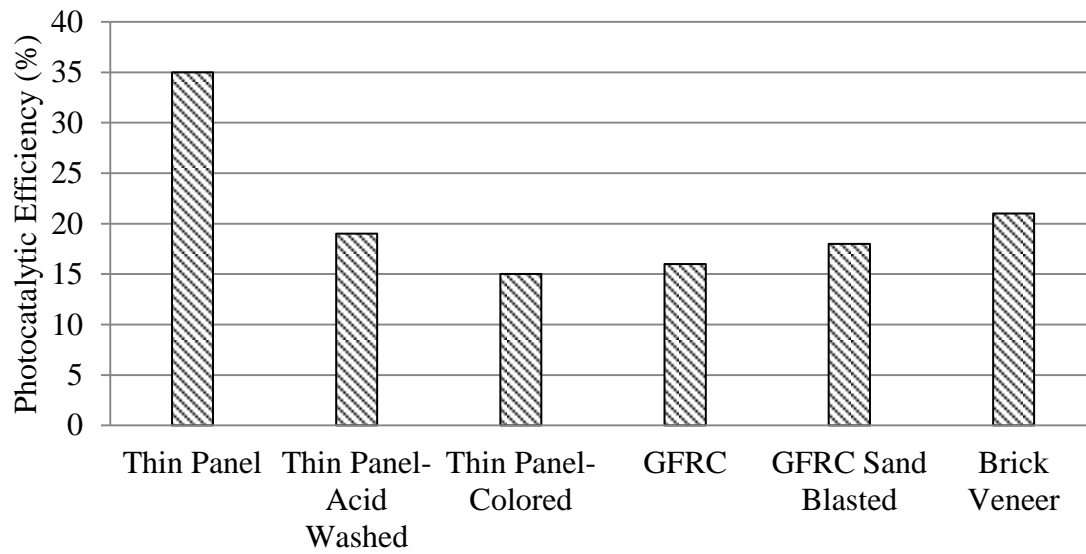


Figure 6.6 Photocatalytic efficiency of specimens from Unlimited Design



Figure 6.7 GFRC panels, no surface treatment (left), media blasted with silica sand (right)

CHAPTER 7

CONCLUSIONS AND FUTURE RESEARCH

7.1 Conclusions

This study tested TiO_2 's effectiveness in reducing NO_x atmospheric pollutants when mixed into a concrete matrix by testing different TiO_2 variables associated with the concrete matrix. The results allowed trends and concerns with this developing technology to be addressed and tested. The following conclusions were determined.

- 1) Not all TiO_2 materials have photocatalytic capabilities to reduce NO_x pollutants. TiO_2 in the anatase phase that were manufactured specifically to be photocatalytic were the only TiO_2 materials tested that had the ability to significantly decrease NO_x pollutant concentrations.
- 2) The higher the quantity of TiO_2 particles per unit area, the higher the photocatalytic efficiency. However, when TiO_2 is mixed into a concrete matrix, there is a plateau effect near 10% TiO_2 by cement mass. The fineness of the TiO_2 particles makes the concrete mixture stickier, which may require changes to the mixture design to maintain workability.
- 3) UV irradiance is a dominating variable, with higher UV irradiances leading to higher photocatalytic efficiencies. The UV irradiance that reaches a typical building façade year round is strong enough for the photocatalytic TiO_2

mechanism to occur. The rate of chemical reaction, rate of diffusion, and the area of the sample all play a role in the kinetics leading to the apparent photocatalytic efficiency of a specimen. Apparent photocatalytic efficiency increases when the NO_x pollutant concentration decreased and when the flow rate decreases. The difference in apparent efficiency between 0.3 ppm and 1.0 ppm stays relatively consistent for all three flow rates tested.

- 4) To reduce the additional cost of using TiO₂ in a mixture design, a lift system where only the lift is exposed to the atmosphere works equally as well to using TiO₂ throughout the thickness of the concrete element. However, if high levels of vibrations are used for compaction, a dilution effect may occur if the layer containing TiO₂ is thin.
- 5) Media blasting, sanding, and acid etching of new specimen's dislodge the TiO₂ particles, reducing the specimen's photocatalytic efficiency.
- 6) The photocatalytic efficiency of concrete specimens that contain photocatalytic TiO₂ significantly decreased when exposed to weather for 120-days. The season and orientation of the testing regiment did not significantly change the effect of being exposed to weather. The decrease in photocatalytic efficiency of the weathered specimens is possibly due to the increase rate of carbonation of the concrete surface. The concrete carbonation reaction generates calcium carbonate, which increased the density of the concrete matrix as well as covers the TiO₂ particles, leading to less TiO₂ particles available for the NO_x oxidation cycle.
- 7) Rejuvenation techniques for the weathered specimens including power washing, media blasting, acid washing and sanding were investigated. Acid washing the

surface was the most effective rejuvenation technique with a rejuvenation performance of 60% the initial photocatalytic efficiency.

A correlation exists between tropospheric ozone generation and NO_x air pollutants. The UV irradiation provided by the sun is strong enough to cause a photocatalytic reaction in TiO₂. If used on a large scale through construction building materials, there is a possibility to reduce the concentration of NO_x pollutants and therefore reduce tropospheric ozone concentrations.

7.2 Future Research

The developing technology for concrete containing TiO₂ is progressing; however, more research and testing needs to occur before it is ready for large spread use. Three areas need to be addressed in future research studies.

The first area includes developing a technique to increase the long-term photocatalytic efficiency of concrete surfaces that contain TiO₂. This will be important as owners weigh the advantages of including this technology and the cost increase in their new construction projects. It will also be a requirement to show the benefit longevity if this technology is to encourage the U.S. Green Building Council to award LEED points for using this technology.

The second area involves testing mixture designs that utilize TiO₂ and supplementary cementitious materials. Supplementary cementitious materials are often required by specifications and their interaction is unknown. There may be potential to reduce the carbonation rate of the concrete, which may increase the long-term photocatalytic performance of the surface.

The final area of future research involves gaining a better understanding of what influence implementing this technology could have on the NO_x and tropospheric ozone concentrations if used on a small or large scale. These studies should include predictors for relative humidity, average temperatures, NO_x pollution concentrations, wind speeds, and UV intensities.